THE PENNSYLVANIA STATE UNIVERSITY
SCHREYER HONORS COLLEGE

DEPARTMENT OF KINESIOLOGY

MEASUREMENT OF ARM SWING ASYMMETRY USING VIDEO-BASED MOTION ANALYSIS AND ACCELEROMETRY

NANCY CAMPBELL
Spring 2012

A thesis
submitted in partial fulfillment
of the requirements
for a baccalaureate degree
in Kinesiology
with honors in Kinesiology

Reviewed and approved* by the following:

Stephen J. Piazza
Associate Professor of Kinesiology
Thesis Supervisor and Honors Advisor

Jinger S. Gottschall
Assistant Professor of Kinesiology
Honors Advisor
Second Reader

* Signatures are on file in the Schreyer Honors College.

ABSTRACT

For chronic and progressive illnesses, such as Parkinson's disease, early disease detection can be crucial in delaying the advancement of symptoms and preventing early death. Recent research has suggested the use of arm swing asymmetry as one criterion to be used in Parkinson's diagnosis. It is unknown, however, which method is the most sensitive detector of arm swing asymmetry. In this study, a perturbation, in the form of unequal wrist weights, was used to induce arm swing asymmetry in ten normal, healthy college students. Arm motion was detected using video-based motion analysis and accelerometers, and arm swing was quantified as excursion of the wrist, forearm accelerations computed from video-based motion analysis, and forearm accelerations obtained from accelerometers. Approximately one and a half strides of steady-state walking data were analyzed in each trial. The areas under receiver operator characteristic curves indicated that accelerations from marker data were the most sensitive detectors of arm swing changes in response to the applied perturbations. Analyses of variance and post-hoc mean comparisons showed that increasing the mass added to the wrist resulted in decreases in arm swing and that women had larger arm swings than men.

TABLE OF CONTENTS

Chapter 5: Discussion

LIST OF FIGURES

LIST OF TABLES

ACKNOWLEDGEMENTS

First, I would like to thank Dr. Stephen Piazza for the tremendous amount of time and effort he took to help me throughout both my thesis and the Schreyer Honors College process. He wrote all of the code in Matlab, and ensured that I understood what was being done in every step. I really appreciate his guidance and patience over the past four years.

I would also like to thank Nori Okita for teaching me how to use the Motion Analysis system and helping out with any problems I encountered, both in data collection and processing. I'd like to thank Mike Kelly for helping me get my data processed quickly and correctly.

Finally, a big thanks goes to my family and friends for always being supportive and patient when I needed them, especially my Mom, Kristen, and Wes. Their endless encouragement has kept me sane.

CHAPTER 1

INTRODUCTION

1.1 Statement of the Problem

For chronic and progressive illnesses, early disease detection can be crucial in delaying the advancement of symptoms and preventing early death. One such example is Parkinson's disease (PD). PD is a motor disorder caused by the death of brain cells that produce dopamine, a neurotransmitter that aids in human movement. PD currently affects over 500,000 people in the United States, and has an average age of onset of 60 years old. With the average age of the population on the rise, the number of people affected by the disease is expected to increase in coming years (Pollack, 2005).

The exact cause of PD is unknown, and positive diagnosis is made only after motor abilities are affected. Primary motor symptoms of PD include tremor, limb or trunk stiffness, bradykinesia, and postural instability (Rajput et al. 1997). While historically, the focus of most PD research has been the lower extremity, the decrease or loss of arm swing in PD patients has recently gained attention. Nieuwboer et al. (1998) found that reduced arm swing was the most frequently reported motor dysfunction in PD patients. Furthermore, Wood et al. (2002) discovered that either unilateral or bilateral loss of arm swing was an independent predictor for falls in PD patients. Regardless of the diagnostic criteria used to assess PD, it has been shown that earlier drug treatment can delay mortality (Rajput et al. 1997). For these reasons, the quantification of arm swing asymmetry in PD patients has lately been sought as a means of both early detection and disease monitoring.

1.2 Related Work

Arm swing asymmetry quantification in PD patients was studied Lewek et al. (2010). Different walking conditions were compared between patients early in the progression of PD and controls: normal walking, fast walking, and heel-walking. The researchers examined both arm swing magnitude and arm swing asymmetry, and found, surprisingly, that there were no significant differences between controls and PD patients regarding arm swing magnitude. Arm swing asymmetry, however, was significantly greater in those with PD compared to controls for all conditions. Interestingly, while arm swing asymmetry showed significant differences between controls and PD patients, the researchers found no asymmetry in lower extremity movements for PD patients. This is important because it suggests that asymmetry of arm swing may precede asymmetry of the lower extremity. The researchers concluded that arm swing asymmetry may be useful and reliable as diagnostic or monitoring criteria for PD. To quantify arm swing, Lewek et al. (2010) calculated arm swing as the excursion of the wrist with respect to the origin of the pelvis as detected by video-based motion analysis during a single stride. This method was not compared to others to assess validity, and wrist excursion was the only measure used to characterize arm swing.

Huang et al. (2011) also examined arm swing asymmetry in PD. The researchers confirmed the results found by Lewek et al. (2010): that arm swing asymmetry is significantly higher in PD than controls. Additionally, Huang et al. (2011) determined that there is also significantly reduced bilateral coordination in PD; this was thought to contribute to the detected asymmetry. In this study, forearm angular accelerations, as detected by accelerometer units attached to each forearm, were used to quantify arm swing over approximately 360 strides. While the measurements from accelerometers

were found to be in agreement with results obtained from other methods of gait analysis, the researchers did not directly compare the use of accelerometers to video-based motion analysis, or the use of forearm angular accelerations to other measurements of arm swing, such as wrist excursion.

Roggendorf, et al.(2012) used ultrasound-based motion analysis to measure arm swing asymmetry in two groups of PD patients and controls during treadmill gait. It was again found that arm swing asymmetry was significantly greater in those with PD compared to controls; however the asymmetry in PD patients was greater for those in the early stages of the disease compared to later stages. Arm swing was characterized by shoulder joint angles as detected by an ultrasound motion analysis system. The researchers did not compare this technique to others.

Despite the fact that research has shown repeatedly that arm swing asymmetry is prevalent in early PD and should be used as diagnostic criteria, there are currently no studies in which the methods of arm swing measurement are directly compared in terms of their sensitivity to, or ability to detect, asymmetry. Also, it should be noted that while studies cited above focus on Parkinson's disease, better quantification of asymmetry has the potential to improve the diagnosis of any illness in which arm swing asymmetry is a symptom. Examples of such diseases include stroke, cerebral palsy, and adult onset primary cervical dystonia (Ford et al., 2007; Meyns et al., (2011); Kagi et al., 2008).

1.3 Objectives of the Project

The purpose of this study was to determine if dynamic forearm accelerations measured by accelerometers are a more sensitive method of measuring arm swing asymmetries than either the extent of wrist excursion or the forearm acceleration as detected by video-based motion analysis. The study involved inducing arm swing

asymmetries by applying wrist weights of varying masses. Data obtained from both accelerometers and video-based motion analysis were analyzed.

1.4 Specific Aims of the Project

- Measure wrist excursion using markers and video-based motion analysis.
- Calculate forearm accelerations through differentiation of position data obtained from markers and video-based motion analysis.
- Use accelerometers to directly measure dynamic forearm angular accelerations.
- Perturb symmetry of arm swing with unequal distribution of wrist weights.
- Compare arm swing detected by video-based motion analysis (wrist excursion and forearm accelerations) to arm swing detected by accelerometers (forearm angular accelerations)

1.5 Hypotheses

Hypothesis #1: Accelerometers will be more sensitive detectors of small arm swing asymmetries than excursion measured by video-based motion analysis.

Rationale: Arm swing is caused by the pendular dynamics of the arm modulated by forces generated by muscles acting across the joints of the arm during gait. Newton's Second Law of Motion tells us that the moments generated by muscles contribute directly to arm accelerations. Accelerometers measure those dynamic accelerations, while video-based motion analysis measures the positions of limbs. These positions represent the accumulated

effects of muscle forces, and therefore are expected to be less well suited to detecting minute asymmetries in arm swing.

Hypothesis #2: Arm accelerations measured using accelerometers will be more sensitive detectors of small arm swing asymmetries than accelerations obtained by twice differentiating positions obtained from video-based motion analysis.

Rationale: As mentioned above, accelerations are directly related to torque and the production of arm swing. While accelerometers directly measure accelerations, position data from markers must be differentiated twice to determine accelerations. Marker data is inherently noisy and differentiation is known to magnify this noise. Therefore, it is expected that accelerations calculated from video-based motion analysis will be noisy and, consequently, less well suited to detecting asymmetries than accelerations from accelerometers.

CHAPTER 2

BACKGROUND AND RELATED WORK

2.1 Arm Swing during Walking and the Importance of Measuring Arm Swing Asymmetry

Initially believed to be simply an inherited trait from four-legged ancestors, researchers have proposed many purposes for the pendulum-like motion of arm swing that occurs opposite to leg movements during walking (Ortega et al. 2008). Arm swing during walking is believed to decrease vertical ground reaction moment, reduce lateral displacement of the center of mass, counteract angular momentum of the legs, and increase stability (Collins et al., 2009; Ortega et al., 2008). Arm swing is considered symmetrical when both arms behave identically and perfectly out of phase (Sadeghi et al., 2000). Many clinical conditions alter the symmetry of arm swing and result in detectable side-to-side differences, making arm swing asymmetry potentially useful for disease diagnosis and monitoring.

2.1.1 Arm Swing Asymmetry in Parkinson's Disease

Arm swing may become asymmetrically reduced or absent, and may present as the only symptom of PD for years. As a result, unilateral loss or reduction of arm swing during walking is a useful clinical sign in the detection of PD (Thompson, 2004). In a study by Zampieri et al., (2010) wearable inertial sensors were used to compare 22 gait and postural transition parameters between controls and PD patients during both the traditional Timed Up and Go (TUG) test and a modified version of the TUG. It was found that, of all 22 parameters measured, arm swing showed the largest difference

between the two groups; PD patients demonstrated an asymmetrical reduction in peak arm swing velocity when compared to controls.

A study by Lewek et al. (2010) found that, compared to controls, Parkinson's patients exhibited significantly higher arm swing asymmetry across three different walking conditions. Using a video-based motion system, it was also discovered that when walking velocity increased or walking pattern was altered, arm swing magnitude increased but arm swing asymmetry remained unchanged in PD patients. Interestingly, there appeared to be no asymmetry in lower extremity in the PD patients used in the study. The researchers concluded that arm swing asymmetry, rather than arm swing magnitude, may be a more reliable parameter in the detection of early PD.

Huang et al. (2011) measured arm swing asymmetry in PD patients and controls using wearable accelerometer assemblies on each forearm. The researchers found, in agreement with Lewek et al. (2010), that arm swing asymmetry was significantly higher in PD patients than controls. It was also found that PD patients have reduced bilateral coordination of arm swing compared to controls; this is believed to contribute to the observed asymmetry.

In agreement with both Lewek et al. (2010) and Huang et al. (2011), Roggendorf et al. (2012) found an increase in arm swing asymmetry in Parkinson's patients compared to controls. The researchers also found that arm swing asymmetry was more prevalent in patients in earlier stages of PD compared with patients in later stages. It was discovered that intra-individual arm swing amplitude of both sides was highly correlated in controls, lesser correlated in patients with more progressed PD, and not associated at all for

patients with early stage PD. The researchers concluded that arm swing asymmetry was an accurate predictor for Parkinson's disease status.

2.1.2 Arm Swing Asymmetry in Other Illnesses

In the literature, arm swing asymmetry has been documented as an indication for other diseases as well. In patients with adult onset primary cervical dystonia, the frequency of reduced arm swing was significantly greater than in controls, and in these patients, 86% had reduced arm swing only on one side (Kagi et al., 2008). In children with hemiplegic cerebral palsy, arm swing was also asymmetric. The hemiplegic side demonstrated significantly smaller anterior-posterior arm swing length than the non-hemiplegic side, regardless of walking velocity. Normal children did not show any significant side-to-side differences in arm swing (Meynset al., 2011). Studies in stroke patients also revealed arm swing asymmetry; arm swing amplitude on the non-paretic side was approximately double the arm swing amplitude on the paretic side (Ford et al., 2007).

2.1.3 Arm Swing Asymmetry in Normal Populations

If arm swing asymmetry is to be used as a diagnostic criterion, it is important to understand asymmetries present in the arm swing of normal populations. Cross, Collard & Nelson (2008) found that all normal, healthy subjects without previous upper extremity injury swung one arm more, with differences in hand displacement ranging from 4-29%.

Kuhtz-Buschbeck et al., (2008) studied arm swing asymmetry in young, healthy subjects as well. Arm swing asymmetry, characterized by arm swing amplitude, was present in almost half of the trials, and in 10 of the 16 subjects, direction of asymmetry was predictable regardless of walking velocity. The researchers found that arm swing

asymmetry was independent of handedness and leg movements. It was concluded that some degree of arm swing asymmetry is physiological, and should be taken into account when using arm swing asymmetry to detect pathologies.

Another study by Donker et al. (2002) examined arm swing adaptations in healthy subjects to four different conditions: no perturbation, mass added to both wrists, mass added only to the right wrist, and mass added only to the right ankle. The mass consisted of a 1.8 kg bracelet that was attached with Velcro. The researchers used video-based motion analysis and electromyography (EMG) to calculate forearm angular displacement and muscle activity, respectively. It was discovered that loading both arms resulted in a significant decrease in arm movement and significant increase in muscle activity as compared to the control trial. Loading one arm led to a significant reduction in that arm's movement, an increase in movement of the opposite arm, and a significant increase in the muscle activity of both arms.

2.2 Methods for Measuring Movement

There are numerous methods available in human movement analysis, in terms of technologies used to measure how humans move. Each offers researchers its own benefits and drawbacks in data collection and processing.

2.2.1 Technologies Used to Measure Movement

Human motion analysis has been traditionally performed using a video-based approach. Three-dimensional video-based motion analysis systems are comprised of two or more cameras and at least three reflective markers placed on palpable bony landmarks on the skin. Light-emitting diodes (LEDs) mounted on the cameras send out infrared or invisible light and the cameras record the markers' reflection of these rays. Triangulation

of the marker in space is achieved by locating the best-fit intersection of multiple camera rays for each marker. Through the use of specialized computer software, three dimensional trajectories from the markers are created and labeled (Davis et al., 1991). The marker positions themselves can be used to compute distances and angles, and changes in marker position over time can be used to determine velocities and accelerations. Velocity and acceleration of markers or segments are calculated by differentiation of position and velocity, respectively.

Video-based motion analysis presents some prospective drawbacks. One potential problem is found when differentiating noisy or incorrect data; data noise can be caused by lighting, marker identification problems, electrical interference, movement, or camera placement. Differentiation magnifies these errors, resulting in inaccurate measurements and extensive data processing. Other disadvantages of video-based analysis are the large expense and large amount of space required to set up a multi-camera system. Bernmark & Wiktorin (2002) cite additional shortcomings with optoelectronic and camera based analysis systems. Prior to use, the cameras must be calibrated; after this, it is impossible to move the cameras without recalibration, making it difficult to use in field studies. Markers also have the potential to obstruct human movement.

Accelerometers are another option available for use when studying human movement. Accelerometers used in human motion detection are classified as piezoresistive, piezoelectric, capacitive, or strain gauge. All of these are electromechanical devices that operate as a mass-spring system and make measurements of acceleration using Newton's Second Law of Motion and Hooke's Law. When forces outside the unit produce an acceleration, a mass inside the unit is displaced and the

spring to which it is attached produces a restoring force proportional to the external force. Using the displacement of the mass, the mass itself, and stiffness of the spring, the acceleration can be calculated (Kavanagh & Menz, 2008). Modern accelerometers are considered small micro electro-mechanical (MEMS) devices, simply meaning they are small machines driven by electricity (Andrejasic, 2008). Accelerometers may be uniaxial or multiaxial; they can measure accelerations in one axis or multiple perpendicular axes, respectively.

Accelerometers offer many benefits to researchers. They are low in cost, small, do not obstruct to human movement, and can be used virtually anywhere to collect large amounts of data. Since they measure accelerations directly, no differentiation is required and therefore fewer errors are found in the dynamic accelerations. Through integration, angular velocity and rotation of human segments can be determined. One weakness of accelerometers, however, as described by Kavanagh & Menz (2008) is that their reliability has not been well documented.

Yet another option for researchers to use when measuring human movement is gyroscopes. Gyroscopes operate based on the principles of angular momentum, and directly measure orientation as well as angular velocity. Benefits and drawbacks of gyroscopes are discussed by Aminian et al. (2002). Gyroscopes are small, inexpensive, and can be used outside of the gait laboratory. Angular velocity can be integrated to arrive at rotation angles, or differentiated to calculate angular accelerations. Powerful processing and filtering are required, however, to negate signal drift and artifact.

Ultrasound-based systems are also available to measure human movement. These systems utilize three receivers per body segment of interest to obtain its position and

orientation in space. From this data, the position of other anatomical points relative to the receivers can be calculated as well. During data collection, the transmitter sends out bursts of ultrasound to the markers and the delay it takes to reach the receivers is recorded to calculate position of segments. Based on these spatial coordinates, joint angles and other spatial-temporal gait variables can be measured, such as step length and stride time. The method, however, presents a severe disadvantage in the limited range allowed for use (Kiss et al., 2004).

Electromyography (EMG) is a method used by researchers to measure muscle activity. When skeletal muscle is activated, it generates electrical potential that can be measured by EMG electrodes placed on the skin lying over the muscle of interest. While EMG relays information regarding muscle activation, it is not informative of position or acceleration, as are other methods of measurement.

2.3 Components of Symmetry Measurements

Symmetry measures have two elements: the gait variable and the method used to calculate symmetry. For each component, there are numerous variations used by researchers.

2.3.1 Parameters Used to Measure Arm Movements

There are many different parameters used by researchers to measure arm movements and compare side-to-side symmetry during walking. One such variable is joint angle. Joint angles are described as one segment's orientation in relation to another. Riad et al. (2011) described movement of the upper extremity during walking in terms of joint angles to identify and classify deviations from normal in patients with spastic hemiplegic cerebral palsy; this measure was called arm posture score. The researchers measured four variables: shoulder flexion/extension, shoulder abduction/adduction,

elbow flexion/extension, and wrist flexion/extension. The researchers used markers and a camera-based system to capture these joint angles.

Joint angles were also used by Roggendorf et al. (2012) to measure arm swing. In this study, arm swing was deconstructed into forward and backward swings. Forward arm swing was described as a positive angle between the arm perpendicular and the global horizontal axis, while backward arm swing was represented by a negative angle.

Kuhtz-Buschbeck et al. (2008) investigated the relationship of arm swing asymmetry and handedness. The researchers measured arm swing in terms of the joint angles of the elbow and shoulder, as well as shoulder joint rotation and wrist excursion, which is the distance travelled by the wrist in the anterior/posterior directions. Elbow joint angle was defined as the relationship of markers on the acromion, lateral epicondyle of the humerus, and the styloid process of the ulna; this described flexion and extension of the arm. Shoulder rotation in the transverse plane was calculated as the angular excursion of the right and left acromion processes about the longitudinal axis of the body. For both the shoulder joint angle and wrist excursion, measurements were described relative to a reference line of zero, which was equivalent to when the arm was straight at the subjects' sides. The shoulder joint angle was positive and negative when the elbow was in front of this line and behind it, respectively. Arm swing amplitude was measured by wrist excursion in the anterior and posterior directions relative to the reference line.

Wrist excursion was also used to quantify arm swing magnitude in a study done by Lewek et al. (2010) The researchers defined arm swing as the excursion of the wrist in the anterior, posterior, medial, and lateral directions with respect to the origin of the pelvis.

Similar to wrist excursion is displacement, or the length travelled by a particular point during one complete gait cycle. In a study conducted by Cross et al. (2008) arm swing was defined as hand displacement in space, as measured by a video-based motion system. Meyns et al. (2011) calculated arm swing length by measuring the difference of the maximum and minimum position of a hand marker in the sagittal plane. To confirm the validity of this as a measure of arm swing length, the researchers also measured the angle between the humerus and the vertical axis. It was found that the largest swing lengths, as measured by displacement, also had the greatest upper arm elevation angles; therefore, the researchers considered their method effective.

Another common variable is range of motion. Range of motion was used by Zampieri et al. (2010) to describe the difference between the maximum and minimum movement of the forearms in the longitudinal axis during arm swing. Gyroscopes were used to detect these values. Riad et al. (2011) also measured range of motion as the difference between maximum and minimum position during the gait cycle for each of the four variables measured (shoulder flexion/extension, shoulder abduction/adduction, elbow flexion/extension, wrist flexion/extension). In both studies, range of motion was measured in degrees.

Velocity is yet another parameter useful for measuring arm swing. In a study conducted by Zampieri et al. (2010), arm swing was characterized by peak arm swing velocity, which was calculated as the maximum angular velocity recorded during the swing phase.

Angular displacement is another variable that can be used to quantify arm swing; this method was used by Donker et al. (2002). The researchers recorded the changes in

position of the forearms using a marker-based system. From these data, angular displacement was calculated as the rotational movement in the sagittal plane.

Researchers have also used dynamic angular accelerations to measure arm swing. Huang et al. (2011) achieved this by attaching accelerometer assemblies composed of two accelerometers each onto the forearms of their subjects. Using accelerometers in parallel a known distance apart allowed the cancellation of gravitational accelerations and elbow translation, resulting in the calculation of angular acceleration of each forearm.

2.3.2 Methods Used to Calculate Asymmetries

While asymmetry of gait is often assessed, there is no standard method used to calculate it. Different researchers have proposed, implemented, and compared various techniques to quantify asymmetry.

The symmetry index (SI) represents one common method used to measure symmetry between the left and right sides during human gait (1). This method was proposed by Robinson et al. (1987) to compare a variety of discrete gait variables. In this formula, X_R is the movement of the right limb and X_L the movement of the left. When SI is equal to zero, symmetry is considered perfect between the two sides. A positive SI would signal that the right limb magnitude is greater, while a negative SI would indicate the left limb magnitude is greater.

$$\mathrm{SI} = \frac{(X_R - X_L)}{0.5\,(X_R + X_L)} \times 100\% \qquad (1)$$

The denominator of this formula can be modified; if a study's population is normal, healthy subjects, the reference value is often the average of the two sides, as seen

in (1). If a comparison is being made between injured and uninjured sides, however, the uninjured side is often chosen as the reference value.

The original SI was modified by Karamanidis et al. (2003). The researchers thought that the SI could potentially reduce the real symmetry of subjects; if half of a study's subjects had 10% asymmetry and the other -10%, the mean value would be 0, or no asymmetry, and would not accurately portray the measured asymmetry. To avoid this dilemma, Karamanidis et al. (2003) simply took the absolute value of the difference between the right and left values (2).

$$ASI = \frac{|X_r - X_l|}{\frac{1}{2}(X_r + X_l)} \times 100\%. \quad (2)$$

An asymmetry ratio has also been used to quantify asymmetry of gait parameters (2). According to Sadeghi et al.,(2000) a ratio of one indicates perfect limb symmetry, while values above or below this signify asymmetries in gait on the right and left sides, respectively. Riad et al. (2011) used this method in developing their arm posture index; the researchers divided the pathological side with the non-involved side.

$$R = \frac{X_R}{X_L} \quad (3)$$

Yet another ratio to measure limb symmetry was developed by Vagenas & Hoshizaki (1992) and named the index of asymmetry (Ia) (3). In this formula, the L and R represent the left and right limbs, respectively. The researchers recorded results as 1, 0, or -1; asymmetries larger than 1% were indicated by +/- 1, and a score of 0 indicated perfect symmetry. A similar method was used by Kuhtz-Buschbeck et al. (2008) in

quantifying arm swing asymmetry, although these researchers used a range of +/- 100 instead of a simple trichotomy. Zampieri et al. (2010) and Roggendorf et al. (2012) also used this method to quantify arm swing asymmetry.

$$\mathrm{Ia} = \frac{(L - R)}{\max(L, R)} \times 100 \tag{4}$$

Zifchock et al. (2008) proposed a different method to quantify asymmetry using discrete variables that does not require a reference side: the symmetry angle. The symmetry angle relates to the angle formed by the x-axis and the vector created by plotting the right-side value against the left-side value. Identical values for both the right and left sides would create a vector 45 degrees with respect to the x-axis; this represents perfect symmetry, and can be either positive or negative, depending on the sign of the values. Any deviation from this line indicates asymmetry, and maximum deviations can range +/- 90 degrees. The SA can be converted to percent of the maximum using the formula shown (4). A score of 0 indicates perfect symmetry and 100% describes equal values opposite in magnitude.

$$\mathrm{SA} = \frac{(45^\circ - \arctan(X_{left}/X_{right}))}{90^\circ} \times 100\% \tag{5}$$

Zifchock et al. (2008) compared their SA method to the traditional SI method (1) used to quantify asymmetry, and several drawbacks to the SI were highlighted. The first disadvantage of the SI discussed was in choosing a reference value. When considering healthy subjects with equal asymmetries on opposite limbs, using the left versus right side as the reference offered different results, showing inconsistencies in the SI. The issue of choosing a reference value was also emphasized when subjects are healthy and

normal. Robinson et al. (1987) and Herzog et al. (1989), when faced with this predicament, both used the average of both sides. When Zifchock et al. (2008) employed this method, it resulted in significantly lower SI values compared to when one side was used as a reference. This underscored how researchers could potentially be underestimating asymmetry through their choice of symmetry measure.

The SA has been used to quantify upper extremity asymmetry. This method was employed by Lewek et al. (2010) to quantify arm swing asymmetry in PD patients. For this study, arms were separated not into left and right arm (X_{left}/X_{right}) but instead the arm that swung less and the arm that swung more, as described by wrist excursion. This method was also used by Huang et al. (2011) although minimum and maximum forearm angular accelerations were used instead of arm swung less or more.

CHAPTER 3

METHODOLOGY

3.1 Subjects

Participation in this study was limited to subjects without known musculoskeletal problems or history of injury to the shoulder, wrist, and elbow. Upper extremity injury, whether past or current, could potentially alter arm swing and therefore was used as exclusion criteria. There were ten participants: five males and five females. All were healthy, aged between 18 and 23 years old, and right-handed (as indicated by self-report). Subjects had an average height of 173.4 cm and an average weight of 70.7 kg (Table 3.1).

Table 3.1 Subjects' Characteristics

Subject	Gender	Age	Height (cm)	Weight (kg)	Handedness	BMI (kg/m2)
1	M	19	179.1	96.7	Right	30.1
2	M	21	182.9	79.5	Right	23.8
3	F	21	160.0	56.8	Right	22.2
4	F	19	160.0	61.3	Right	23.9
5	M	23	172.7	65.8	Right	22.1
6	F	21	172.7	61.3	Right	20.6
7	M	22	185.4	79.5	Right	23.1
8	F	21	170.2	63.6	Right	22.0
9	F	18	172.7	61.3	Right	20.6
10	M	23	177.8	80.8	Right	25.6

Subjects were told only that arm movements were being measured with both video-based motion analysis and accelerometers during walking. Subjects were not informed of the study's exact purpose or different weight conditions prior to participation to ensure that results were not affected by unnatural arm swing. Subject recruitment was

performed by word-of-mouth at the Biomechanics Laboratory. IRB approval (#36656) was granted from the Office of Research Protections at Penn State University. Each subject signed an Informed Consent form prior to study involvement and was given a copy for personal records (Appendix A).

3.2 Motion Analysis Methods

To directly measure dynamic accelerations, four triaxial G-Link MEMs accelerometers (Microstrain, Inc.; Williston, VT) were used in this study. Two wearable units were made; each consisted of two accelerometers rigidly mounted ten cm apart on a foam-padded aluminum splint that measured 160 mm x 25 mm x 3 mm (Figure 3.1). The units weighed approximately 150 g each. According to Elble (2005), mounting two accelerometers a known distance apart in parallel negates both gravitational influence and elbow translation and allows angular acceleration in a single plane to be computed (6). In this equation, a_{1T} and a_{2T} are the tangential components of acceleration and L is the distance between the accelerometers (10 cm). The sampling rate used during data collection was 128 Hz from one channel and the output was in A/D units. 128 Hz was chosen as the sampling rate because it was closest to the frequency of the video-based motion system (100 Hz).

$$\alpha = \frac{a_{2T} - a_{1T}}{L} \tag{6}$$

Prior to each subject arrival in the laboratory, the accelerometers were calibrated. A digital level was used to determine that the surface used for calibration was level within 0.1 degree. Accelerometers were placed both right side up and upside down for approximately one second. Using these data and gravitational acceleration (9.81 m/s^2), a

linear fit to these two data points calculated the conversion from A/D units to accelerations in m/s^2 (Huang et al. 2011).

Figure 3.1 Mounted accelerometer design

Video-based motion analysis was used to measure arm swing as well. Six Motion Analysis Corporation Eagle digital cameras (Motion Analysis Corp,; Santa Rosa, CA) recorded the movement of markers and, through the Motion Analysis Eagle Hub, the three-dimensional capture volume was created (Figure 3.2). EVaRT 5.0 software was used to capture marker data at 100 Hz.

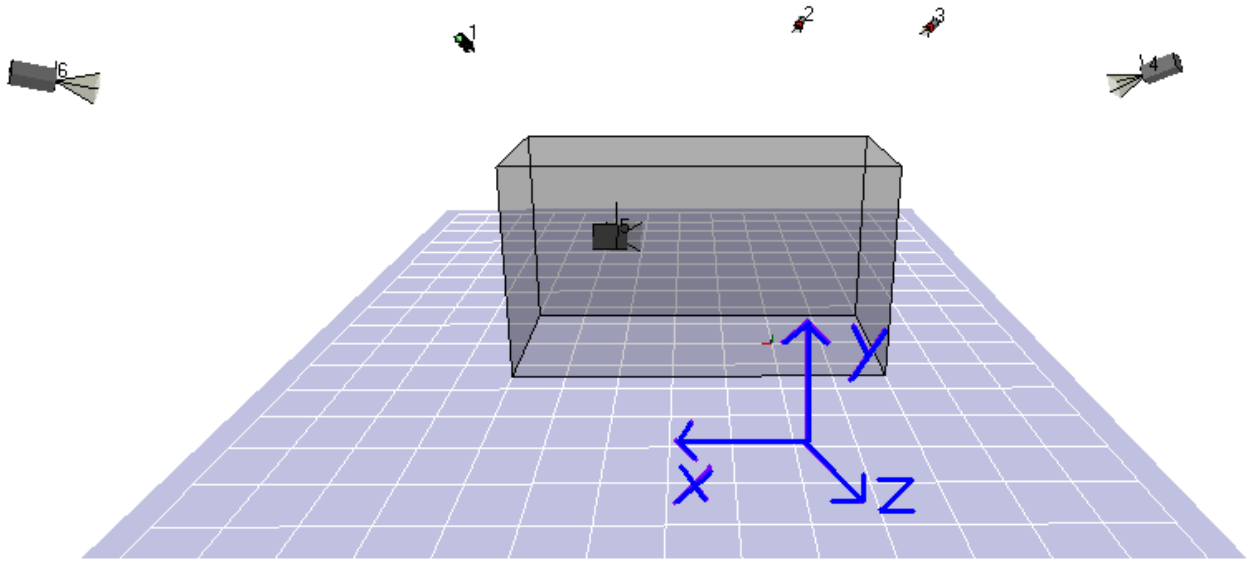

Figure 3.2 Motion Analysis camera set-up and coordinate system

3.3 Protocol

Data collection was performed solely at the Biomechanics Laboratory. Prior to subject arrival, a code written in Matlab 7.11.0 was used to generate the random order of ten different conditions (Table 3.2). Upon subject arrival, informed consent was obtained and informed consent forms were signed. Height and weight were recorded, and no history of upper extremity injury was confirmed. Handedness was self-reported by subjects. Subjects performed two standing trials; the first was used to generate an anatomical coordinate system and the second created a template for the subsequent walking trials. During both, only marker data were collected using the camera-based system.

Table 3.2 Ten different wrist weight conditions

Condition	Mass Left (g)	Mass Right (g)
1	0	0
2	400	0
3	350	50
4	300	100
5	250	150
6	200	200
7	150	250
8	100	300
9	50	350
10	0	400

For the first standing trial, two markers were placed directly on the sides of each accelerometer, totaling four markers per accelerometer unit. Reflective markers were placed on several anatomical landmarks on both the left and right side: the styloid processes of the ulna and radius, both medial and lateral epicondyles of the humerus, and the anterior and posterior superior iliac spines. A pelvic cluster comprised of four markers was attached to the lower back. Bias markers were positioned on the right upper forearm, the left wrist, and the right lower back to help the software discriminate between the left and right sides. Similar to protocol used in a study by Huang et al. (2011), accelerometers were attached to the upper forearms in alignment with the long axis of the forearm and parallel to the dorsum of the hand when the wrist was anatomically neutral. Subjects were instructed to stand in anatomical position with straight elbows and wrists; wrists were then pronated 90 degrees. Three seconds of this static pose was captured **(**Figure 3.3**)**.

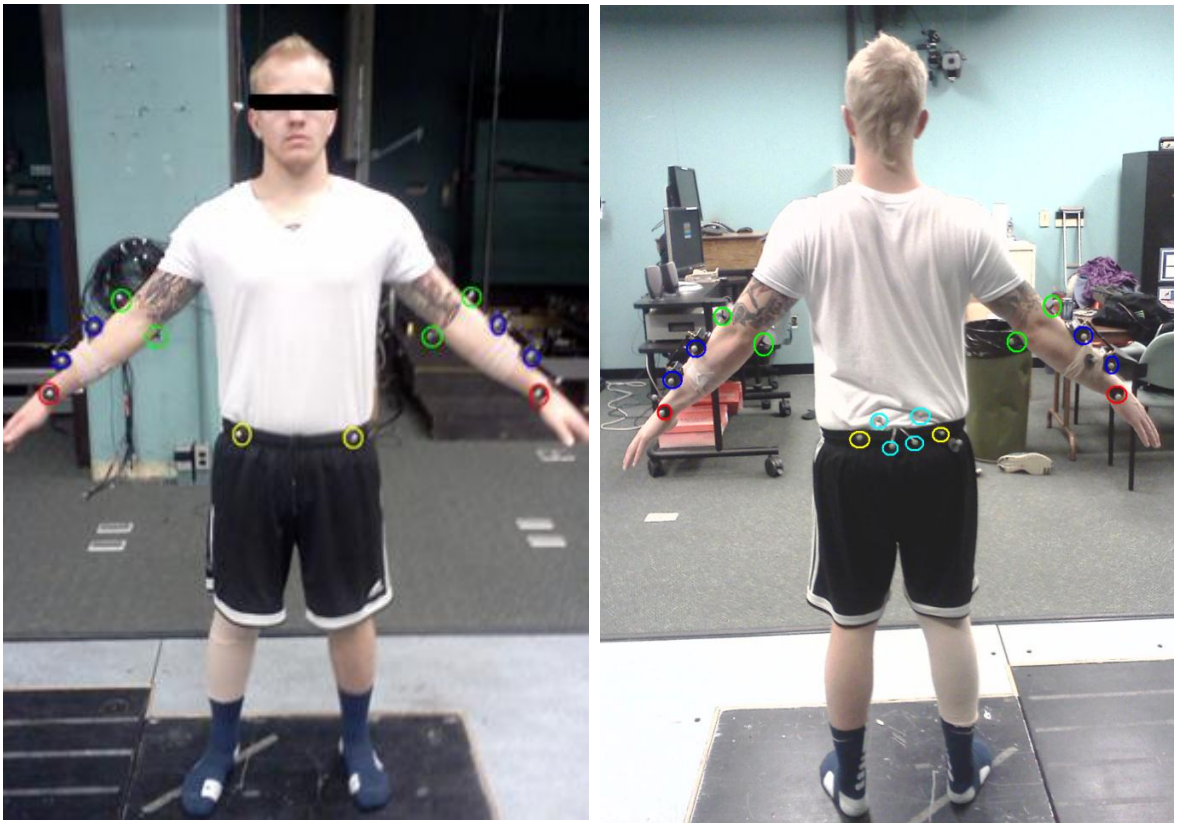

Figure 3.3 Static pose with anatomical landmark markers. In this picture, the markers enclosed by green, red, and yellow circles are anatomical markers that were removed during walking trials. Markers surrounded by dark blue circles are placed directly on the accelerometer units and remained on the subject for walking trials. Light blue circles enclose the pelvic cluster that also remained on subjects during walking trials.

For the following standing trial, wrist, elbow, and both anterior/posterior superior iliac spine markers were removed. Accelerometer markers, pelvic cluster markers, and bias markers were left on. Again, subjects were instructed to stand with wrists pronated 90 degrees from anatomical position. Three seconds of this static pose was recorded, and markers were labeled to create a template in EVaRT.

Wrist weights were then fastened to the subjects' wrists. Subjects did not know the mass conditions throughout the study. For each motion trial, subjects started at a cone placed approximately five meters from the center of the video-based capturing area;

this was done to ensure that arm swing captured was in steady state. Subjects were instructed to "walk at a brisk and comfortable pace, as if you are walking to class" down the runway to a cone about ten meters away, turn around, and return to the start position (Figure 3.2). Once they reached the start cone, subjects were asked to keep their arms static at their sides for approximately one second before resuming walking. During the trials, the accelerometers continuously recorded data for each condition. It was expected that, if subjects kept their arms still at their sides at the start of each trial, trials would be easy to separate because the start of each trial would show very small accelerations. Each of the ten conditions was repeated for five trials, totaling 50 motion trials. 500 frames of marker data, amounting to five seconds, was manually collected for each trial. As stated above, the accelerometers were programmed to continuously collect data for each condition for three minutes; this was determined sufficient time to complete all five trials of each condition. A total of ten accelerometer readings were collected for each subject.

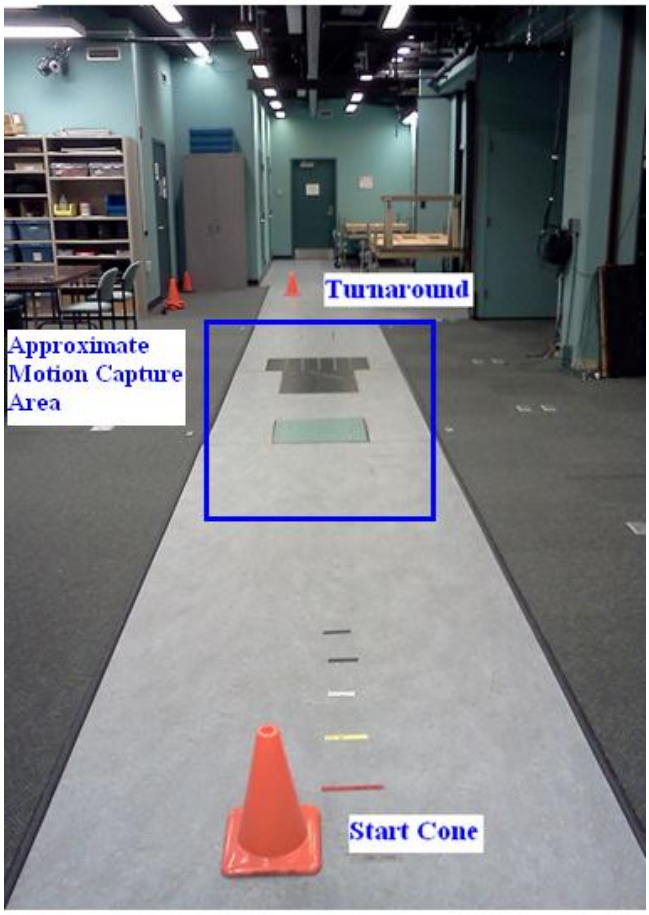

Figure 3.4 Runway area marked with cones for the start and turnaround of each trial and approximate area of motion capture

3.4 Data Analysis

3.4.1 Data Processing

Marker data from the standing and motion trials were loaded into EVaRT 5.0. Gaps in marker trajectories were filled using EVaRT's rigid body function. Once marker data were as complete as possible, a custom program was written in Matlab 7.11.0 to process the data (Appendix B).

The first step in processing the markers was to distinguish between the anatomical markers and the cluster markers in the first standing trial. Anatomical markers were defined as those on the wrists, elbows, and anterior/posterior superior iliac spines

(ASIS/PSIS). There were three marker clusters; the pelvic cluster, and the markers attached to each accelerometer unit on both the right and left forearms. Each cluster was composed of four markers. Three dimensional coordinates of all markers were copied into individual matrices. Anatomical markers were defined for each cluster; for the forearms, anatomical markers included the wrist and elbow markers, while for the pelvis, anatomical markers were those on the ASIS/PSIS.

In order to calculate the location of the cluster markers in the anatomical frame, a series of transformations was used. First, both the anatomical markers and cluster markers were converted from their anatomical and local coordinate systems, respectively, into the global, or laboratory, frame. For the anatomical markers, the origin of each segment (pelvis and left/right forearms) was calculated. For the pelvis, the midpoints of both the right and left ASIS/PSIS were calculated; the midpoint of these midpoints was considered the origin. A similar formula was performed for each forearm using the medial/lateral wrist and elbow. Using these origins, the transformation from the anatomical frame to the global was found for each segment, this was called T_{ga}. For the marker clusters, the first marker was selected as the origin; the transformation from the local coordinate system to the global frame was called T_{gl}.

Next, the transformation from the anatomical coordinate system to the local coordinate system (T_{la}) was calculated by multiplying the inverse of T_{gl} by T_{ga}. The transformation from the local coordinate system to the anatomical coordinate system (T_{al}) was found by taking the inverse of T_{la}. The cluster markers coordinates in the anatomical frame were then calculated and averaged across the middle 200 frames of the first standing trial; this allowed the position of the wrist to be known during motion trials

without using markers on the wrist. Euler angles, wrist position, wrist center, and origin location were all saved. Marker data were low-pass filtered at a cut-off frequency of 7 Hz to remove noise. These data were then double differentiated to produce forearm accelerations; first, angular velocities were computed from finite changes in components of the rotation matrix that described the orientation of each forearm relative to the global coordinate system, and then angular accelerations were computed by numerically differentiating angular velocity vectors.

3.4.2 Accelerometer Data Processing

Custom computer code was written in Matlab 7.11.0 to compute angular accelerations from the raw accelerometer output. To compute angular accelerations, tangential accelerations from the proximal accelerometer were subtracted from those of the distal accelerometer, and this value was divided by the distance between them, which was 10 cm (Elble 2005).

Next, a graph was plotted for each trigger of the left angular accelerations versus time. Since subjects stood with their arms still at their sides prior to beginning each trial, it was clear on the graph where the subjects were standing (angular accelerations were approximately zero) or walking (angular accelerations oscillated about zero). By clicking the graph at the start of each walking trial, the ten accelerometer triggers were separated into fifty trials. Two seconds of steady state acceleration data from each trial were used in statistical analysis.

3.4.3 Statistical Analysis

In this study, changes in arm swing with perturbation were of greater interest than the computation of arm swing asymmetry as previously discussed. When performing

statistical analysis, both wrist excursion (7) and delta wrist excursion (8) from baseline were used. Baseline, $R_{exc(0,0)}$, was the average wrist excursion during the condition in which no weight was added to either wrist. Subtracting the average excursion for each condition in which weights were added from baseline was expected to show changes in arm swing that were induced by the added weight. This approach was also used with accelerations computed from video-based motion analysis and accelerations obtained from accelerometers. In all instances, values computed using (8) were referred to as Δ delta left (Δ_L) and delta right (Δ_R).

$$R_{exc,i} = max_R - min_R \quad (7)$$

$$\Delta_{R,i} = R_{exc(0,0)} - R_{exc,i} \quad (8)$$

A two-way repeated measures analysis of variance (ANOVA) was done in Sigma Stat 3.1 for the following parameters: wrist excursion, accelerations from markers, and standard deviations of accelerations from accelerometers. For each parameter, five ANOVAs was repeated five times: the left arm, the right arm, delta left, delta right, and delta left minus delta right (LMR). Excursions and accelerations were averaged across trials and subjects. The variables of interest were gender and weight condition; gender was included as a factor to account for the possibility that smaller female subjects' arm swings would be affected more by added wrist mass. A post-hoc Tukey tests were run to determine if there were significant differences between the means when ANOVA revealed significant main effects.

Receiver operator characteristic (ROC) curves and area under the curve (AUC) for all asymmetric conditions were generated for delta wrist excursion, delta accelerations from marker data, and delta accelerations from accelerometers in Matlab 7.11.0. ROC

curves are a tool used for displaying the accuracy of a diagnostic test. In this study, a binary classification system of positive and negative was used, and four outcomes were possible (Table 3.3). The four outcomes were: true positive (those who actually have the disease), true negative (those without the disease), false positive (those the diagnosis determine have the disease but truly don't), and false negative (those classified as nondiseased who are actually diseased). For this study, any asymmetric weight conditions were considered diseased, and nondiseased were the conditions in which no mass or equal mass were applied (conditions 1 and 6, respectively). These outcomes are dependent on a threshold; falling above or below this threshold results in a positive or negative diagnosis, respectively. In ROC analysis, sensitivity is considered the true positive rate, while specificity is the true negative rate. ROC curves plot the sensitivity versus the false positive rate, which is one minus the true negative rate.

Table 3.3 Possible outcomes in ROC analysis. In this table, diseased, as characterized by the diagnostic test (P`), is the sum of the true positives and false positives; nondiseased (N`) is the sum of the false negative and true negatives. In reality, the diseased (P) is the sum of the true positive and the false negative, while the nondiseased (N) is the sum of the false positive and true negative. ("2x2 contingency table")

		actual value		
		p	***n***	**total**
prediction outcome	***p'***	True Positive	False Positive	P'
	n'	False Negative	True Negative	N'
	total	P	N	

For an ideal diagnostic test, both sensitivity and specificity would be perfect; this means that test accurately separates subjects into positive and negative, generating no false negatives or false positives. Graphs for perfect tests would have a line extend from (0,0) to (0,1), and then from (0,1) to (1,1) (Figure 3.4). Alternatively, a 45 degree line extending from the bottom left corner to the top right represents complete randomness (Figure 3.4). This line divides the ROC space; points above correspond to a correct diagnosis better than chance, while points below indicate a test that performs worse than random (Figure 3.4).

Area under the curve (AUC) can be used to summarize and compare diagnostic accuracy. To do so, the area between the line of random chance and the line generated by the diagnostic test is computed. The larger the AUC is, the more accurate the diagnostic test used.

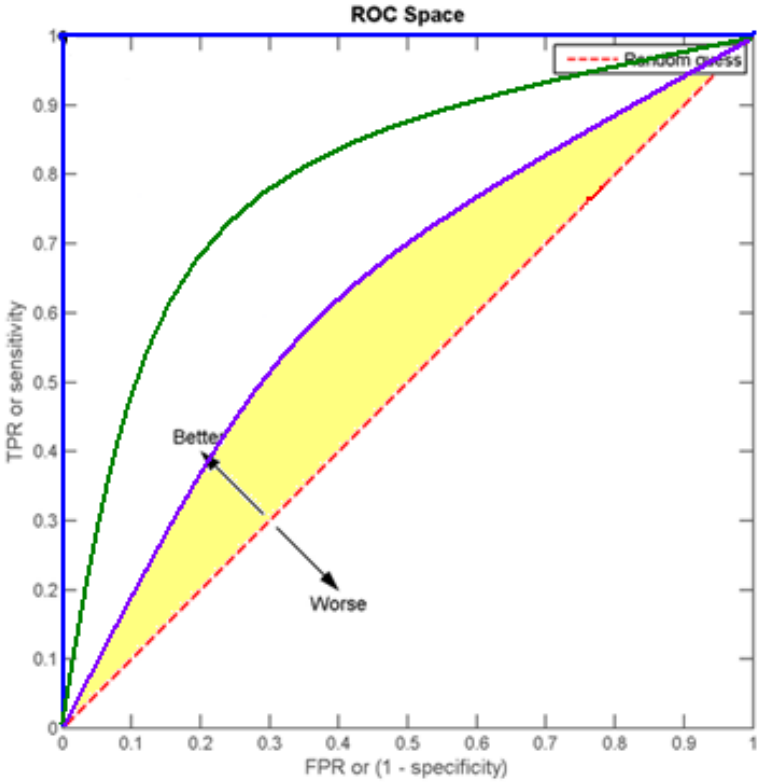

Figure 3.5 ROC curve basic characteristics. In this figure, the red dotted line indicates complete random. Above this line, results are predicted better than chance, while below, results are predicted worse than chance. The purple and green show diagnostic tests that are better than random, while the blue line signifies a perfect diagnostic test. AUC for the purple line is the shaded yellow region.

CHAPTER 4

RESULTS

4.1 Wrist Excursion

There was a significant main effect ($p < 0.001$) of condition on right wrist excursion (Figure 4.1). Post-hoc testing revealed significant differences (all $p \leq 0.049$) for right wrist excursion between the means of condition 10 and conditions 1, 2, 3, 7, and 8 (Figure 4.1; Appendix C). Significant differences ($p = 0.028$) were also found for right wrist excursion between the means of conditions 9 and 2 (Figure 4.1; Appendix C). For left wrist excursion, no significant main effects of condition on were found ($p > 0.05$). Gender was not statistically significant ($p = 0.07$) for both left and right wrist excursions; however, women had larger wrist excursions on both sides.

Regarding the delta wrist excursions, a significant main effect of condition was again found on the right ($p < 0.001$) but not the left ($p > 0.05$). For right delta wrist excursion, significant differences (all $p \leq 0.05$) between the means of condition 10 and conditions 2, 3, 7, and 8 were again found, as well as between the means of conditions 9 and 2 (Appendix C). Gender was not statistically significant ($p > 0.05$) for either left or right delta wrist excursions.

Condition was also found to have a significant main effect ($p < 0.001$) on delta left wrist excursion minus the delta right wrist excursion (LMR). Significant differences (all $p \leq 0.025$) between the means of condition 9 and conditions 2, 3, 4, and 6 were seen as well (Appendix C). Again, gender was not statistically significant ($p > 0.05$).

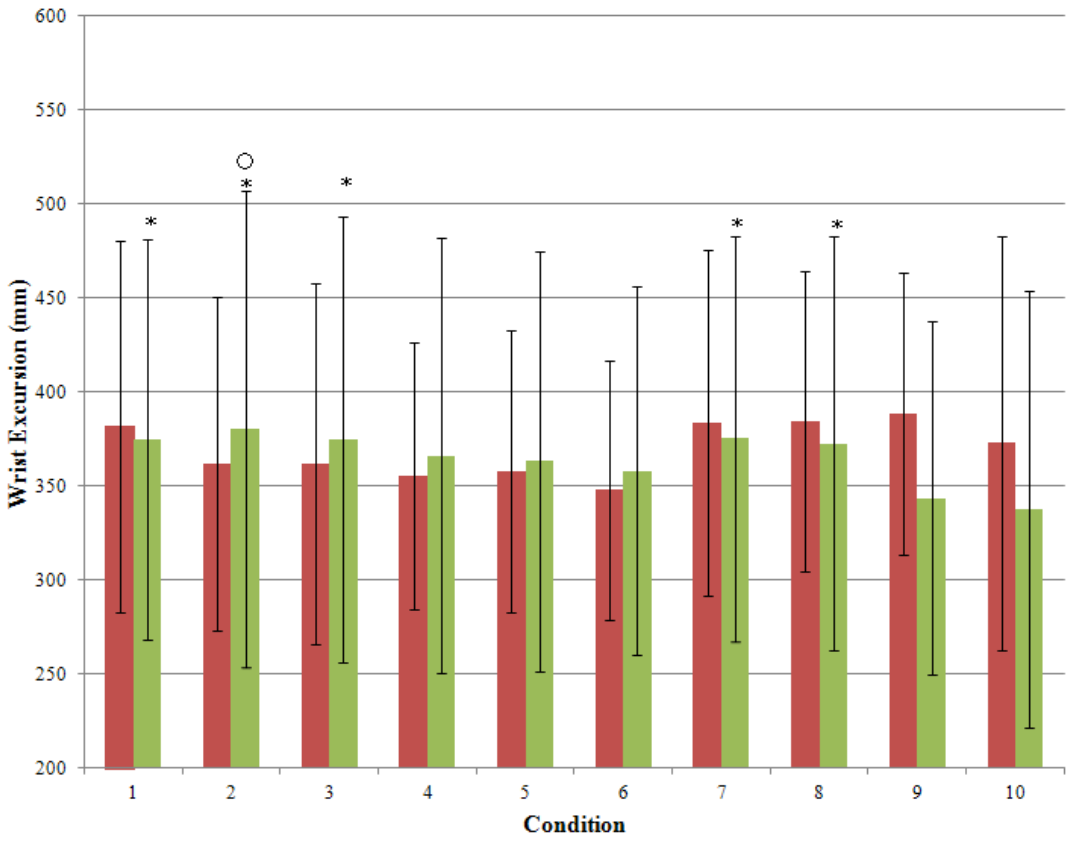

Figure 4.1 Left/right wrist excursions averaged across trials and subjects versus condition. Red bars represent the left arm and green bars represent the right arm. * indicates significant differences (all $p \leq 0.049$) for the right wrist excursion between the means of condition 10 and conditions 1, 2, 3, 7, and 8. ^{O} denotes significant differences ($p = 0.028$) for the right wrist excursion between the means of conditions 9 and 2. Bars indicate one standard deviation from the mean.

ROC curves for all asymmetric conditions were created using delta wrist excursions and AUC were calculated. AUC for asymmetric conditions in which there was a 400 gram difference between wrists was 0.0423 (Figure 4.2). AUC for the 300 gram difference conditions was 0.901 (Figure 4.3). AUC for the 200 gram difference conditions was 0.0327(Figure 4.4). AUC for conditions in which weight difference was 100 grams was -0.0045 (Figure 4.5). AUC versus perturbation condition was graphed (Figure 4.6).

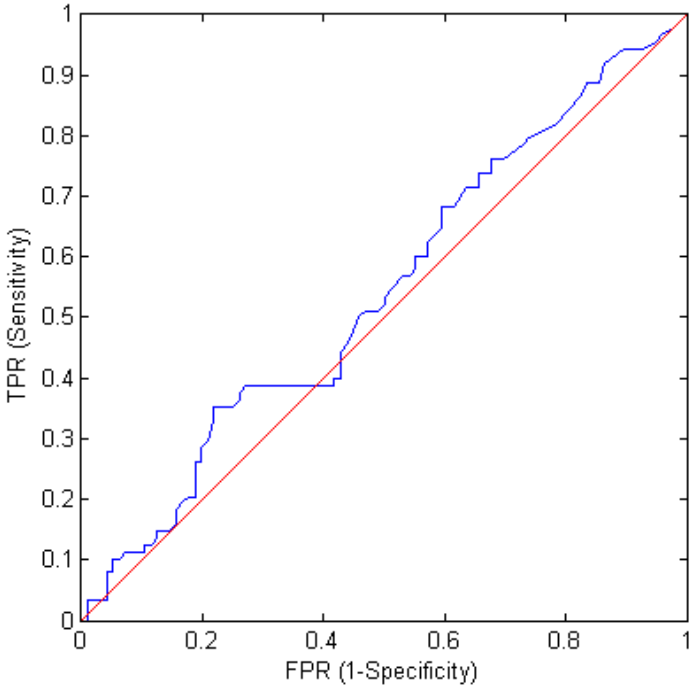

Figure 4.2 ROC curve for delta wrist excursion conditions with 400 gram difference (conditions 2 and 10). The red line represents random guessing. AUC = 0.0423.

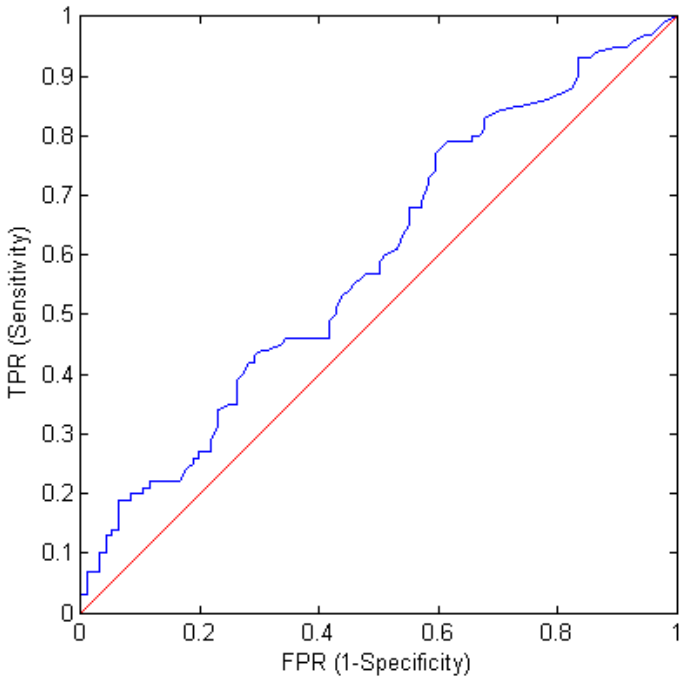

Figure 4.3 ROC curve for delta wrist excursion conditions with 300 gram difference (conditions 3 and 9). The red line represents random guessing. AUC = 0.0901.

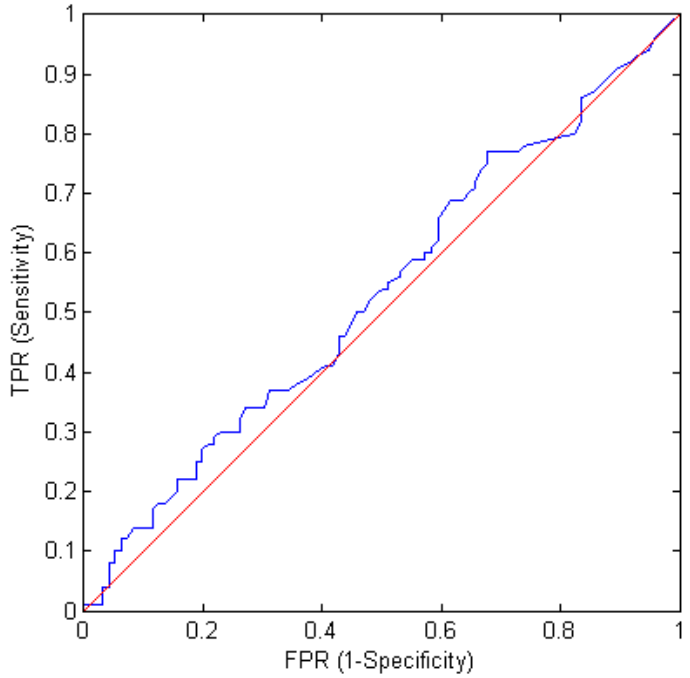

Figure 4.4 ROC curve for delta wrist excursion conditions with 200 gram difference (conditions 4 and 8). The red line represents random guessing. AUC = 0.0327.

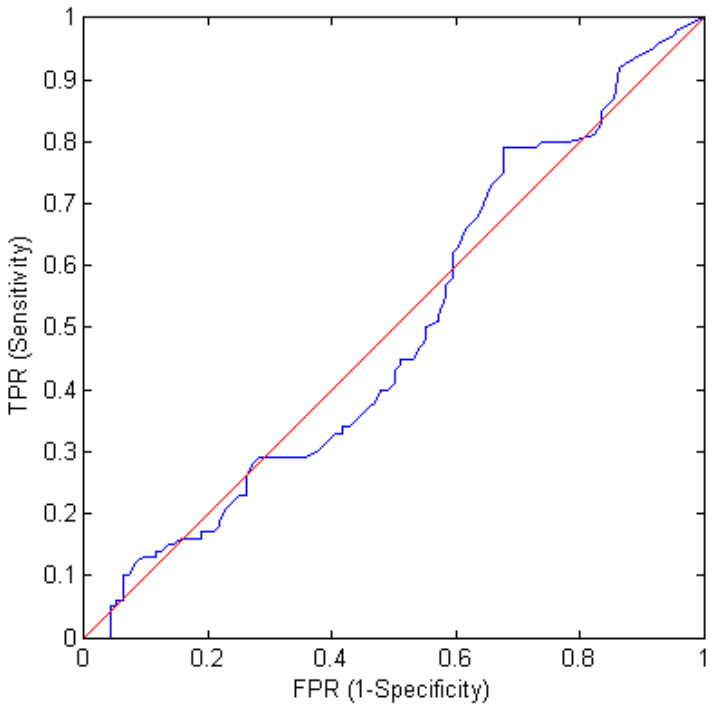

Figure 4.5 ROC curve delta in wrist excursion conditions with 100 gram difference (conditions 5 and 7). The red line represents random guessing. AUC = -0.0045.

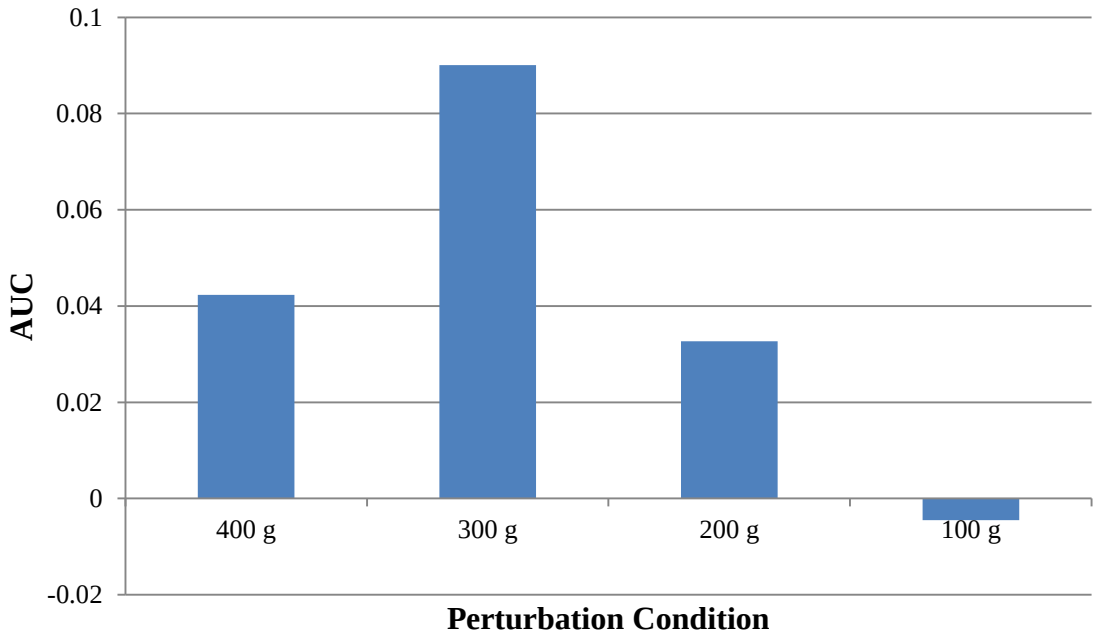

Figure 4.6 AUC versus perturbation condition for wrist excursion. The largest AUC was found for conditions 3 and 9, in which there was a 300 g difference between wrists. A negative area was found for conditions 5 and 7. During these conditions, a difference of only 100 g was present.

4.2 Accelerations from Video-Based Motion Analysis

A significant main effect of gender ($p = 0.026$) on right forearm angular accelerations calculated from marker data was found, indicating that women have larger forearm angular accelerations than men. No main effect for gender was found for the left arm ($p > 0.05$). No significant effects of condition were found on either right or left arm angular accelerations (Figure 4.7).

No significant main effects of either gender or condition were found for delta right, delta left, or LMR ($p > 0.05$).

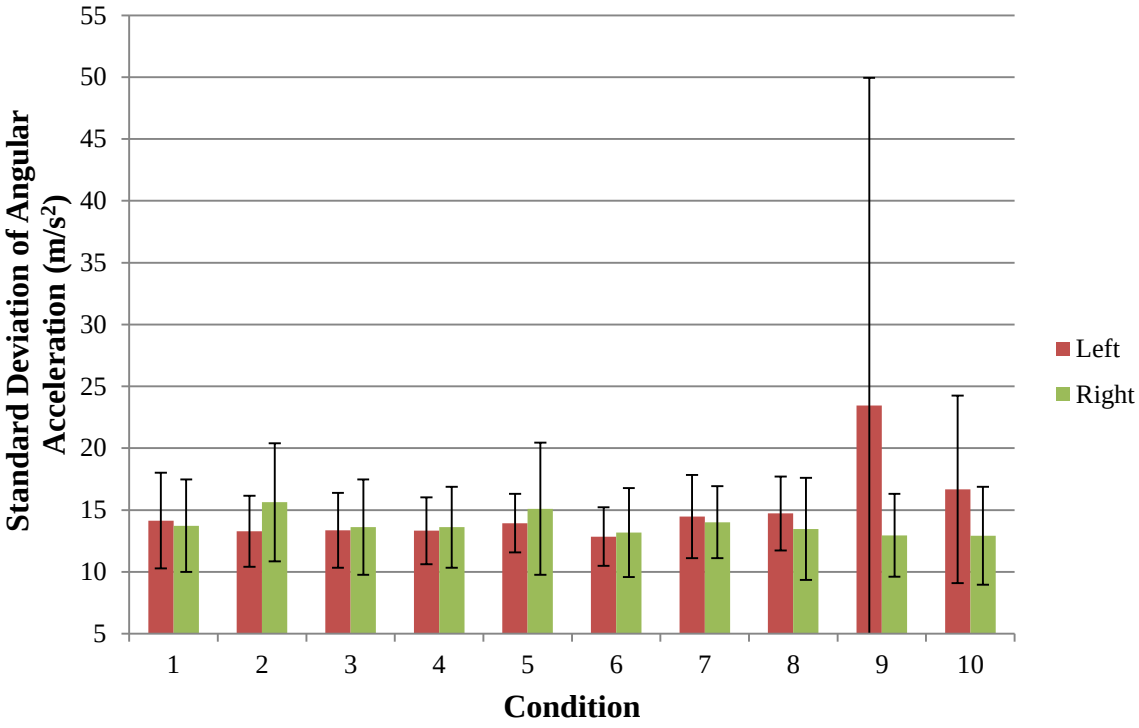

Figure 4.7 Left/right forearm standard deviation of angular accelerations obtained from marker data averaged across trials and subjects versus condition. Bars indicate one standard deviation from the mean.

ROC curves for all asymmetric conditions were created using delta angular accelerations and AUC were calculated. AUC for the most asymmetric conditions in which there was a 400 gram difference between wrists was 0.1557 (Figure 4.8). AUC for the 300 gram difference conditions was 0.0957 (Figure 4.9). AUC for the 200 gram difference conditions was 0.0793(Figure 4.10). AUC for conditions in which weight difference was 100 grams was 0.0351 (Figure 4.11). AUC versus perturbation condition was graphed (Figure 4.12)

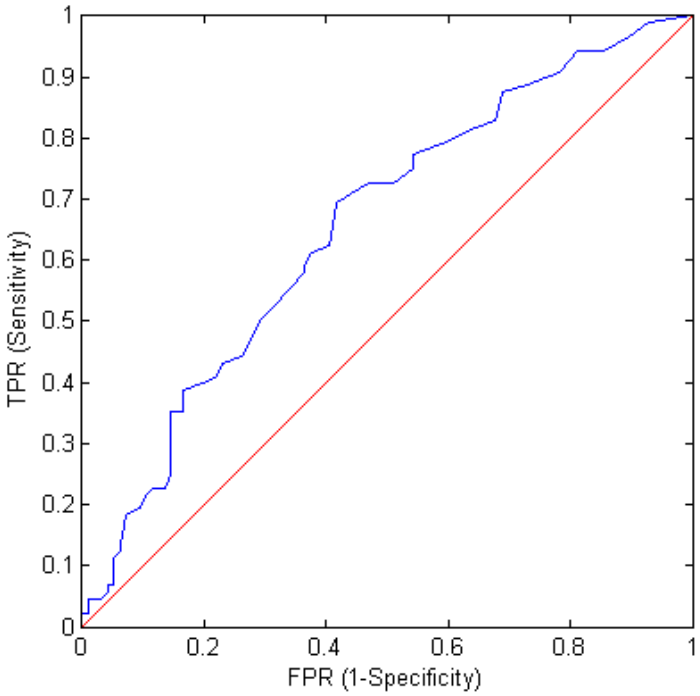

Figure 4.8 ROC curve for delta angular acceleration obtained from marker data for conditions with 400 gram difference (conditions 2 and 10). The red line represents random guessing. AUC = 0.1557.

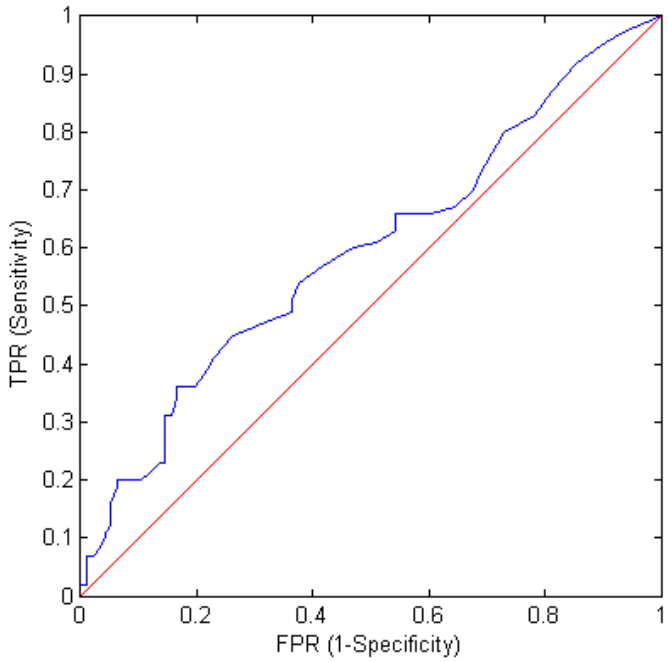

Figure 4.9 ROC curve for delta angular acceleration obtained from marker data for conditions with 300 gram difference (conditions 3 and 9). The red line represents random guessing. AUC = 0.0957.

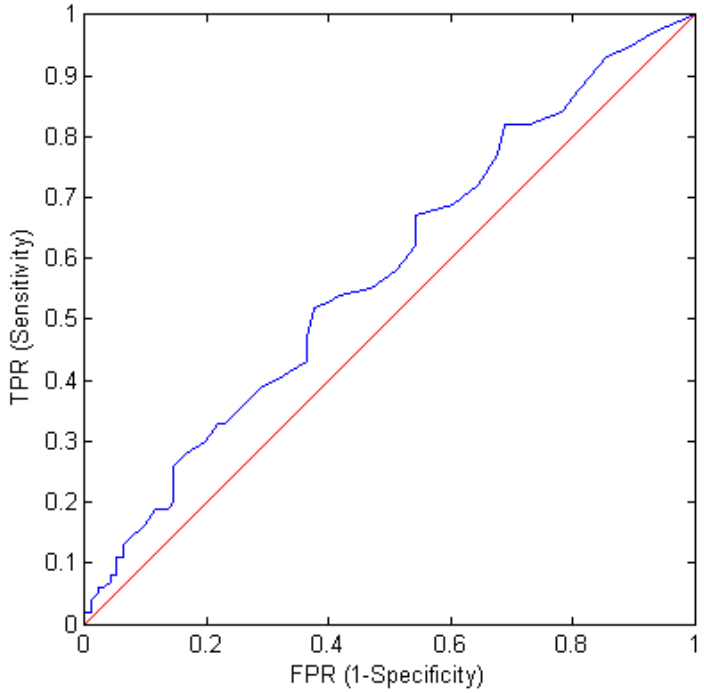

Figure 4.10 ROC curve for delta angular acceleration obtained from marker data for conditions with 200 gram difference (conditions 4 and 8). The red line represents random guessing. AUC = 0.0793.

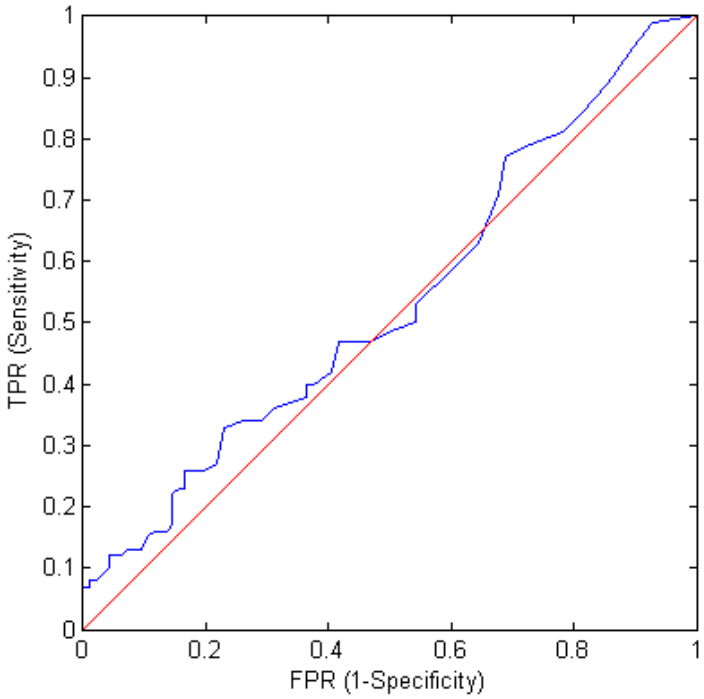

Figure 4.11 ROC curve for delta angular acceleration obtained from marker data for conditions with 100 gram difference (conditions 5 and 7). The red line represents random guessing. AUC = 0.0351.

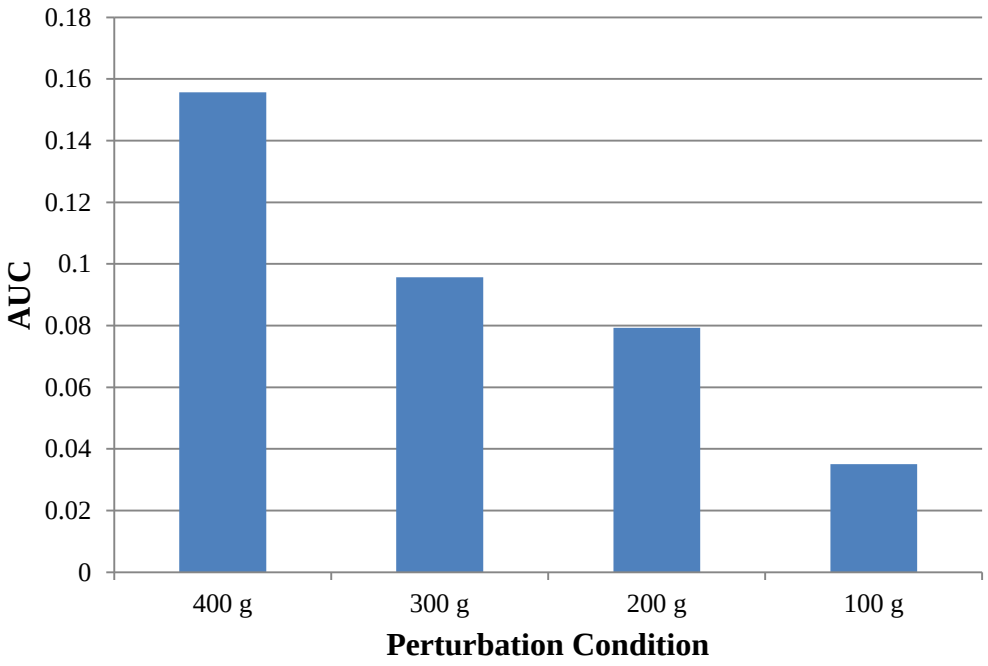

Figure 4.12 AUC versus perturbation condition for angular acceleration obtained from marker data. The largest AUC was found during conditions in which there was a 400 g difference between wrists (2 and 10). The smallest AUC was calculated for conditions in which a 100 g difference was applied (5 and 7).

4.3 Accelerations from Accelerometers

Condition exhibited a significant main effect ($p < 0.001$) on left angular accelerations obtained from accelerometers (Figure 4.13). Significant differences (all $p \leq 0.039$) were found between the means of condition 9 and conditions 2, 3, 4, and 6, as well as between the means of condition 2 and conditions 1 and 10 (Figure 4.13' Appendix C). No significant effect of condition on right forearm accelerations were found ($p > 0.05$).

Additionally, a significant main effect of gender on left forearm angular accelerations was also found ($p = .015$), which again demonstrated larger forearm angular accelerations for women compared to men. No such effect was found for the right forearm.

When examining delta angular accelerations, a significant main effect of condition was again found only on the left ($p < 0.001$). Significant differences (all $p \leq 0.032$) were found between the means of condition 9 and conditions 2, 3, 4, and 6, as well as between conditions 2 and 10 (Appendix C). No main effects of gender were found for either the delta left or delta right accelerations.

There was a significant main effect for condition on LMR ($p = 0.008$). Significant differences (all $p \leq 0.045$) were found between the means of condition 9 and conditions 2, 3, and 6 (Appendix C). Gender was not found to have a significant main effect ($p > 0.05$).

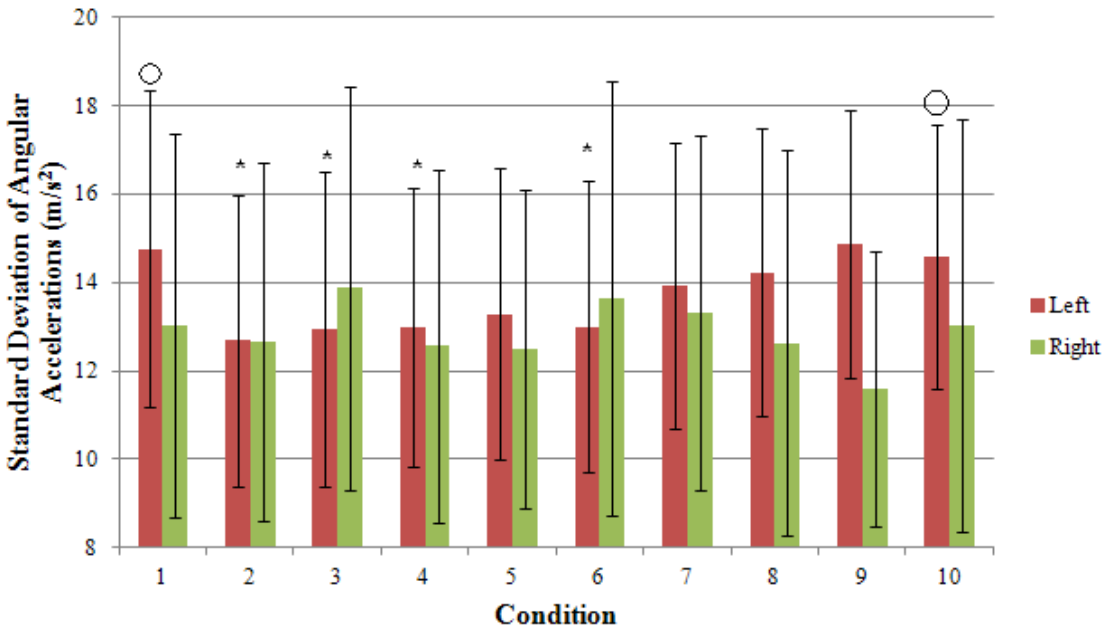

Figure 4.13 Left/right forearm standard deviation of angular accelerations obtained from accelerometers averaged across trials and subjects versus condition. * indicates significant differences (all $p \leq 0.039$) for the left angular accelerations between the means of condition 9 and conditions 2, 3, 4, and 6. ^{O} denotes significant differences (all $p \leq 0.039$) for the left angular accelerations between the means of condition 2 and conditions 1 and 10. Bars indicate one standard deviation from the mean.

ROC curves for all asymmetric conditions were created using delta angular accelerations and AUC computed. AUC for conditions in which there was a 400 gram difference between wrists was 0.1535 (Figure 4.14). AUC for the 300 gram difference conditions was 0.0298 (Figure 4.15). AUC for the 200 gram difference conditions was 0.0677(Figure 4.16). AUC for conditions in which weight difference was 100 grams was 0.0177 (Figure 4.17). AUC versus perturbation condition was graphed (Figure 4.18).

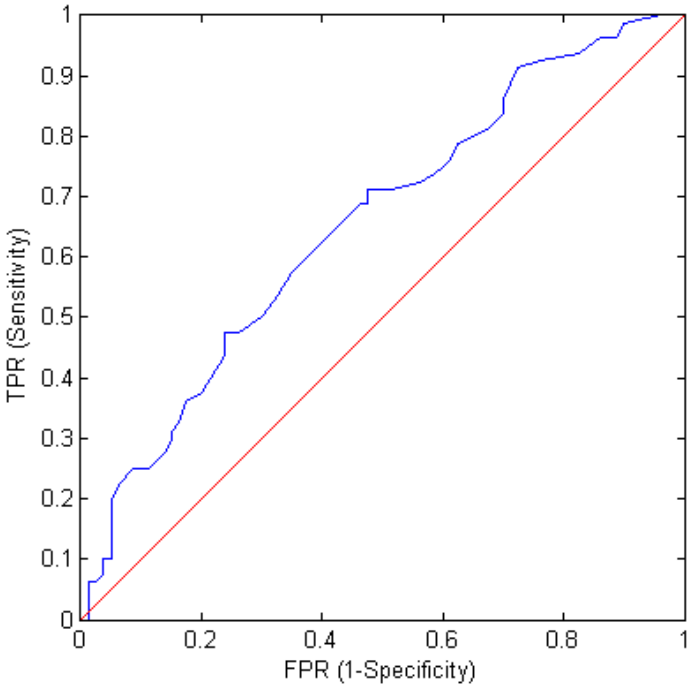

Figure 4.14 ROC curve for delta angular accelerations obtained from accelerometers for conditions with 400 gram difference (conditions 2 and 10). The red line represents random guessing. AUC = 0.1535.

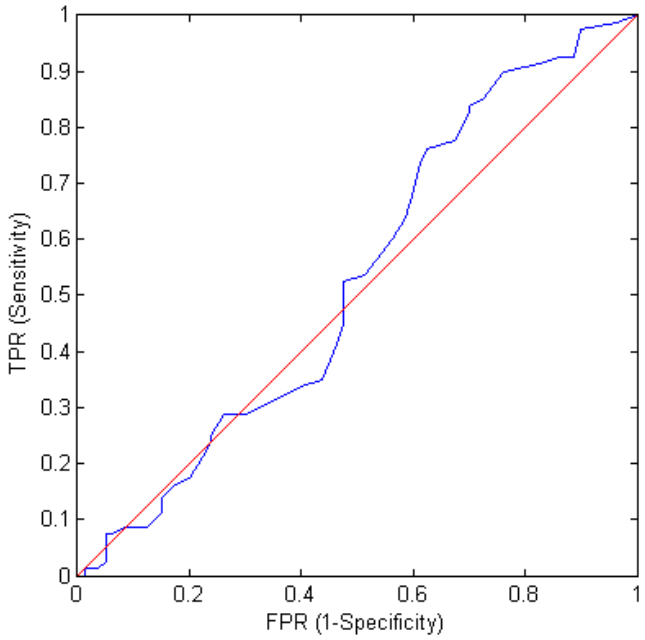

Figure 4.15 ROC characteristic curve for delta angular acceleration obtained from accelerometers for conditions with 300 gram difference (conditions 3 and 9). The red line represents random guessing. AUC = 0.0298.

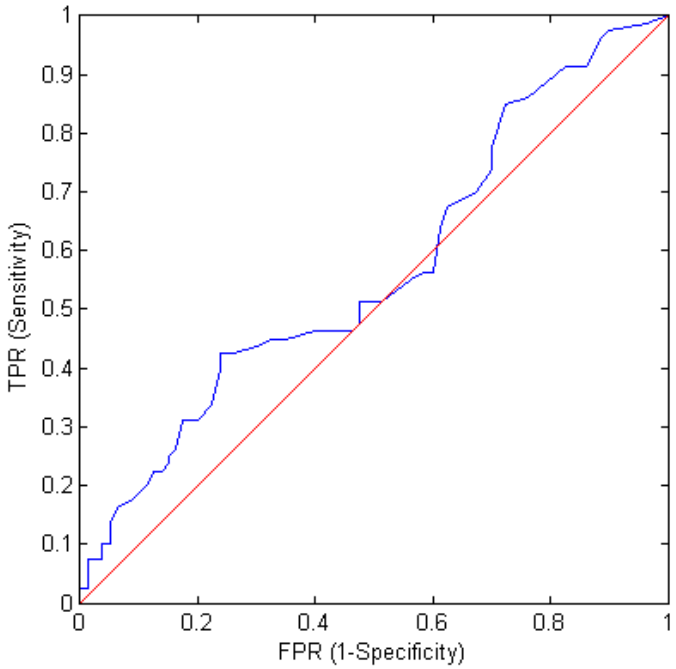

Figure 4.16 ROC curve for delta angular acceleration obtained from accelerometers for conditions with 200 gram difference (conditions 4 and 8). The red line represents random guessing. AUC = 0.0677.

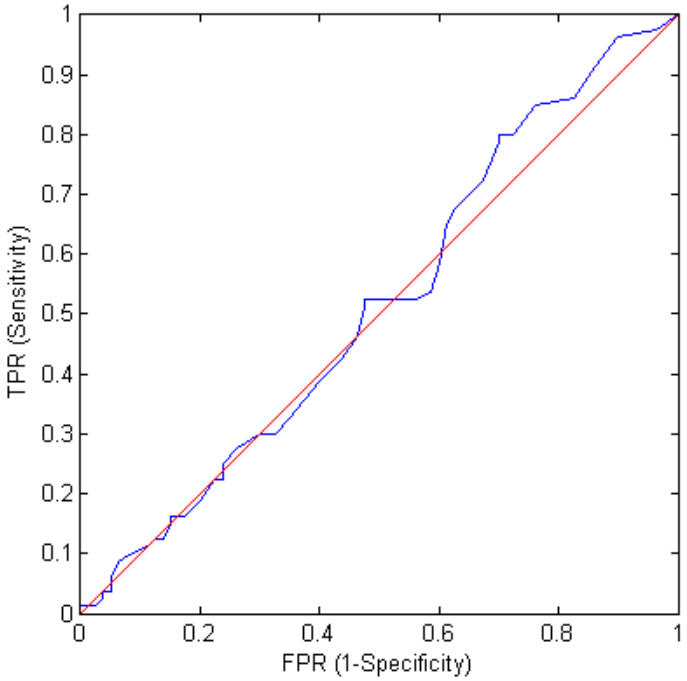

Figure 4.17 ROC curve for delta angular acceleration obtained from accelerometers for conditions with 100 gram difference (conditions 5 and 7). The red line represents random guessing. AUC = 0.0177.

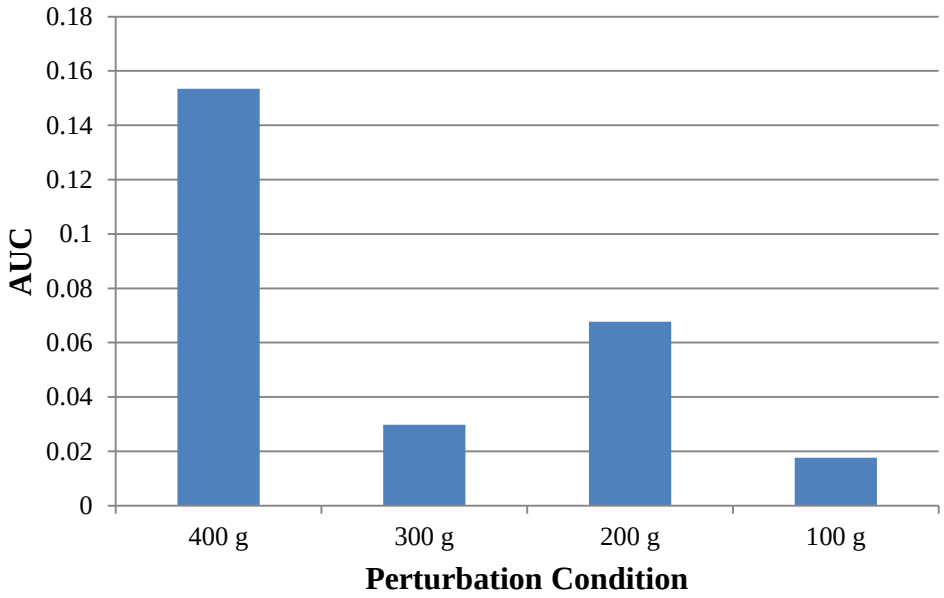

Figure 4.18 AUC versus perturbation condition for accelerations obtained from accelerometers. The largest AUC was computed for conditions in which a 400 g difference was added (2 and 10). The smallest AUC was found for conditions that had a 100 g difference between wrist weights (5 and 7).

CHAPTER 5

DISCUSSION

5.1 Key Findings

Of the methods used, the largest AUC was found when a 400 g difference in wrist weights was applied and accelerations from video-based motion analysis were used to measure arm swing (Figure 4.8). The AUC for this condition was slightly smaller for accelerations from accelerometers, and the smallest AUC was measured when wrist excursion was used to detect arm swing (Figure 4.14, Figure 4.2). Additionally, it was expected that, as the magnitude of perturbation increased, the ability to detect it would increase as well. This was true only for accelerations from video-based motion analysis (Figure 4.12). Neither wrist excursions nor accelerations from accelerometers displayed this predicted relationship between the magnitude of perturbation and sensitivity in detection (Figure 4.6, Figure 4.18). Consequently, of the methods used to measure arm swing, accelerations seemed more sensitive than wrist excursions at detecting perturbation, as predicted. Contrary to expectation, however, accelerations from video-based motion analysis proved more sensitive than those from accelerometers.

This study also revealed an unexpected influence of gender on arm swing; a significant main effect was found for accelerations from both marker data and accelerometers, and a trend toward significance was found for wrist excursion. In all instances, it seemed that women had larger arm swings, even without normalizing data for height.

The main effects for condition on wrist excursion and accelerations from accelerometers agreed with predictions (Figure 4.1, Figure 4.13). For both methods, it

appeared that increasing mass on one arm resulted in decreased motion of that arm, as expected.

5.2 Comparison to Previous Findings

Kuhtz-Buschbeck et al. (2008) also quantified arm swing in young, healthy subjects using wrist excursion in the anterior/posterior directions. At self-selected walking speeds, the researchers found the average lengths of left and right arm swing were 35.9 cm and 31.4 cm, respectively. In this study, comparable values were found; average left arm swing was 38.2 cm and average right arm swing was 37.4 cm when arm swing was quantified by wrist excursions during condition 1 (no mass was added to either the left or right sides; Figure 4.1).

Similarly, Huang et al. (2011) quantified arm swing in PD subjects and healthy controls using the standard deviation of forearm angular accelerations detected by accelerometers. For the PD subjects, arm swing ranged from about 10 to 20 (m/s^2), and controls ranged from approximately 20 to 30 (m/s^2). In this study, standard deviation of accelerations from both accelerometers and marker data ranged from about 10 to 20(m/s^2; Figure 4.7, Figure 4.13). Although these subjects were young and healthy, the arm swings that were measured were more consistent with the PD subjects from Huang et al. (2011) than healthy controls. This could be a result of the perturbations that were introduced in this study.

According to Hosmer & Lemeshow (2000), AUC between 0.2 and 0.3 is acceptable discrimination, AUC between 0.3 and 0.4 indicates excellent discrimination, and AUC above 0.4 signifies outstanding discrimination, however values this high are extremely rare. In this study, the highest AUC, which was obtained using accelerations

from video-based motion analysis during the 400 g difference conditions, was 0.1557 (Figure 4.6). This suggests that none of the methods used provide adequate discrimination between asymmetric and symmetric conditions (which represented our "disease" and "nondisease" conditions). It is also possible that decreased AUC results from perturbations that were not large enough to consistently alter arm swing.

In past research, Kozlowski & Cutting (1977) found, based only on observation, that, "female walkers had a more pronounced arm swing than males." This agrees with findings from the current study, in which all three methods used to measure arm swing detected that females have a larger arm swing than males. This research provides the first quantitative description of gender differences in arm swing.

Donker et al. (2002) demonstrated that adding mass to one wrist decreased arm swing on the perturbed side and increased movement of the opposite arm. The current study also showed that asymmetrically increasing mass results in decreased motion of that arm. It was not found, however, that motion of the opposite arm consistently increased in response to added weight. This could be attributed to differences in mass used between the studies. Donker et al. (2002) applied a 1.8 kg bracelet, while this study only applied a maximum of 400 g.

5.3 Implications of Results

Findings of this study indicate that accelerations are more sensitive than wrist excursions at detecting perturbations in arm swing. A possible explanation of this observation is that accelerations are more closely related to the forces that produce arm swings than positions, increasing their sensitivity at detecting changes in arm swing. Additionally, only accelerations obtained from video-based motion analysis displayed a

relationship between the magnitude of perturbation and sensitivity of perturbation detection (Figure 4.12). This justifies their use in future research investigating changes in arm swing in response to either perturbation or disease.

Another interesting discovery was that women have a larger arm swing than men, despite the fact that they were, in this study, shorter. During walking, arm swing counteracts the angular momentum of the legs and trunk that occurs with each step. It is possible that the larger arm swing observed in women is due to differences in both anatomy and walking dynamics between males and females. Compared to men, women, in general, have larger hips, and also exhibit greater hip sway when walking. The larger arm swing of women, then, could be a response to an increased angular momentum of the trunk due to these noted differences.

Both accelerometers and video-based motion analysis detected significant decreases in arm swing with increased mass (Figure 4.1, Figure 4.13). As stated above, arm swing serves to counteract the angular momentum of the legs and trunk during walking. Angular momentum is the product of angular velocity and moment of inertia. Adding mass to one wrist changes the moment of inertia for that arm. One explanation for the observed decrease in arm swing with added mass could be that, by changing the moment of inertia of one arm, that arm is able to counteract the angular momentum of the trunk with a smaller swing. Alternatively, it is also possible that adding mass reduces arm swing because of the increased effort required to fully swing a weighted arm.

5.4 Limitations of this Study

One of the largest limitations of the study was the length of walking data analyzed, which was a little more than one stride. While accelerometers are able to

record more data than this, the video-based motion analysis range has a limited area for data collection; this is a well-known short-coming of video-based motion analysis. Consequently, only approximately one and a half full strides were available for data analysis from this method. To keep comparisons equal between the technologies, accelerometer data was shortened to approximately one and a half strides as well.

Another limitation of this study relates to the amount of mass added to the wrists. Pilot testing suggested that 400 grams was enough to perturb arm swing but these data were collected with a lean female as the sole subject. If pilot data had been collected using a more muscular subject, perhaps a larger male, it is possible that we would have realized that 400 grams would not be enough mass to alter arm swing. Another option might have been to use percent body weight of each subject to determine the amount of weight applied; this would have normalized the perturbation for each subject.

Subjects in this study were all right-handed. While previous work has suggested that arm swing is not affected by handedness, there is the possibility that there is a relationship between the two (Kuhtz-Buschbeck et al., 2008). A study population consisting of equal numbers of right- and left-handed subjects would have provided a more universal application of results.

Walking velocity during this study was not controlled. Although subjects received instruction regarding appropriate velocity, velocity was self-selected. It has been documented that faster walking velocity generates a larger magnitude of arm swing (Donker et al., 2002; Lewek et al. 2010; Roggendorf et al. 2012). It is probable, therefore, that subjects with a faster self-selected walking speed swung their arms more.

While this was known prior to data collection, self-selected walking speed was chosen, rather than controlling for velocity, to try and measure arm swings as natural as possible.

5.5 Conclusions

This was the first study to compare the sensitivity of wrist excursions, accelerations from video-based motion analysis, and accelerations from accelerometers to changes in arm swing in response to perturbation. Results indicated that accelerations computed from marker data were most sensitive to the effects of perturbation magnitude on arm swing. It was also found that women had larger arm swings than men, despite the fact that they were shorter. Future directions of research may include:

- Comparison of wrist excursion, accelerations from video-based motion analysis, and accelerations from accelerometers to detect arm swing asymmetry in subjects with PD and controls.
- Investigation of the differences in arm swing between men and women using more subjects.
- A repeat of this experiment using larger differences in mass to create more detectable changes in arm swing.
- Repeating this experiment with equal numbers of right- and left-handed subjects to explore the effect of limb dominance on adaptation to weight.

REFERENCES

(n.d.). *2x2 contingency table*. [Web Graphic]. Retrieved from http://en.wikipedia.org/wiki/Receiver_operating_characteristic

Aminian, K., Najafi, B., Bula, C., Leyvraz, P. F., & Robert, P. (2002). Spatio-temporal parameters of gait measured by an ambulatory system using minature gyroscopes. *Journal of Biomechanics, 35*(5), 689-699.

Andrejasic, M. University of Ljubljana, Department of physics. (2008). *Mems accelerometers*

Bergmann, J., Mayagoitia, R., & Smith, I. (2009). A portable system for collecting anatomical joint angles during stair ascent: A comparison with an optical tracking device. *Dynamic Medicine, 8*(3), doi: 10.1186/1476-5918-8-3

Bernmark, E., & Wiktorin, C. (2002). A triaxial accelerometer for measuring arm movements. *Applied Ergonomics*, *33*(6), 541-547.

Collins, S., Adamczyk, P., & Kuo, A. (2009). Dynamic arm swinging in human walking. *Proceedings of the Royal Society B,* 3679-3688.

Cross, A., Collard, M., & Nelson, A. (2008). Body segment differences in surface area, skin temperature and 3d displacement and the estimation of heat balance during locomotion in hominins. *Public Library of Science*, *3*(6), e2464.

Davis, R., Ounpuu, S., Tyburski, D., & Gage, J. (1991). A gait analysis data collection and reduction technique. *Human Movement Science*, *10*, 575-587.

Donker, S. F., Mulder, T., Nienhuis, B., & Duysens, J. (2002). Adaptations in arm movements for added mass to wrist or ankle during walking. *Experimental Brain Research*, *146*(1), 26-31.

Elble, R. (2005). Gravitational artefact in accelerometric measurements of tremor. *Clincal Neurophysiology, 116*(7), 1638-1643.

Ford, M., Wagenaar, R., & Newell, K. (2007). Phase manipulation and walking in stroke. *Journal of Neurologic Physical Therapy, 31*, 85-91.

Herzog, W., Nigg, B., Read, L., & Olsson, E. (1989). Asymmetries in ground reaction force patterns in normal human gait. *Medicine and Science in Sports and Exercise, 21*(1), 110-114.

Hosmer, D.W. & Lemeshow, S. (2000) *Applied logistic regression,* 2nd edn. John Wiley & Sons, New York.

Huang, X., Mahoney, J., Lewis, M., Guangwei, D., Piazza, S., & Cusumano, J. (2011). Both coordination and symmetry of arm swing are reduced in Parkinson. *Gait & Posture,* doi: 10.1016/j.gaitpost.2011.10.180

Kagi, G., Schwingenschuh, P., & Bhatia, K. (2008). Arm swing is reduced in idiopathic cervical dystonia. *Movement Disorders, 23*(12), 1784-1787.

Karamanidis, K., Arampatzis, A., & Bruggemann, G. (2003). Symmetry and reproducibility of kinematic parameters during various running techniques. *Medicine & Science in Sports & Exercise, 35*(6), 1009-1016.

Kavanagh, J., & Menz, H. (2008). Accelerometry: A technique for quantifying movement patterns during walking. *Gait & Posture, 28*(1), 1-15.

Kiss, R.M., Kocsis L., & Knoll Z. (2004). Joint kinematics and spatial-temporal parameters of gait measured by an ultrasound-based system. *Mechanical Engineering & Physics, 26*(7), 611-620.

Kozlowski, L., & Cutting, J. (1977). Recognizing the sec of a walker from a dynamic point-light display. *Perception & Psychophysics, 212*(6), 575-580.

Kuhtz-Buschbeck, J. P., Brockmann, K., Gilster, R., Koch, A., & Stolze, H. (2008). Asymmetry of arm-swing not related to handedness. *Gait & Posture, 27*(3), 447-454.

Lewek, M., Poole, R., Johnson, J., Halawa, O., & Huang, X. (2010). Arm swing magnitude and asymmetry during gait in the early stages of Parkinson's disease. *Gait & Posture, 32*(2), 256-260.

Meyns, P., Van Gestel, L., Massaad, F., Desloovere, K., Molenaers, G., & Duysens, J. (2011). Arm swing during walking at different speeds in children with cerebral palsy and typically developing children. *Research in Developmental Disabilities, 32*(5), 1957-1964.

Ortega, J., Fehlman, L., & Farley, C. (2008). Effects of aging and arm swing on the metabolic cost of stability in human walking. *Journal of Biomechanics, 41*(16), 3303-3308.

Pollack, M. (2005). Intelligent technology for an aging population: The use of AI to assist elders with cognitive impairment. *AI Magazine, 26*(2), 9-24.

Nieuwboer, A., Weerdt, W., Dom, R., & Lesaffre, E. (1998). A frequency and correlation analysis of motor deficits in Parkinson patients. *Disability and Rehabilitation, 20*(4), 142-150

Rajput, A. H., Uitti, R., Rajput, A., & Offord, K. (1997). Timely levodopa administration prolongs survival in Parkinson's disease. *Parkinsonism & Related Disorders, 3*(3), 159-165.

Riad, J., Coleman, S., Lundh, D., & Brostrom, E. (2011). Arm posture score and arm movement during walking: A comprehensive assessment in spastic hemiplegic cerebral palsy. *Gait & Posture, 33*(1), 48-53.

Robinson R.O., Herzog W., Nigg B.M. (1987). Use of force platform variables to quantify the effect of chiropractic manipulation on gait symmetry. *Journal of Manipulative and Physiological Therapeutics, 10*(4), 172-176.

Roggendorf, J., Chen, S., Baudrexel, S., van de Loo, S., Seifried, C., & Hilker, R. (2012). Arm swing asymmetry in Parkinson's disease measured with ultrasound based motion analysis during treadmill gait. *Gait & Posture, 35*(1), 116-120.

Sadeghi, H., Allard, P., Prince, F., Labelle, H., (2000) Symmetry and limb dominance in able-bodied gait: A review. *Gait & Posture,12*(1), 34-45.

Thompson, P. (2004). Clinical neurological assessment of balance and gait disorders. In A. Bronstein, T. Brandt, M. Woollacott & J. Nutt (Eds.), *Clinical Disorders of Balance, Posture and Gait* (pp. 93-98). London: Arnold.

Vagenas, G., & Hoshizaki, B. (1992). A multivariable analysis of lower extremity kinematic asymmetry in running. *International Journal of Sport Biomechanics, 8*(1), 11-29.

Wood, B. H., Bilclough, J. A., Bowron, A., & Walker, R. W. (2002). Incidence and prediction of falls in parkinson's disease: A prospective multidisciplinary study. *Journal of Neurology, Neurosurgery, and Psychiatry, 72*(6), 721-725.

Zampieri, C., Salrian, A., Carlson-Kuhta, P., Aminian, K., Nutt, J., & Horak, F. (2010). The instrumented timed up and go test: potential outcome measure for disease modifying therapies in Parkinson's disease. *Journal of Neurology, Neurosurgery, and Psychiatry, 81*(2), 171-176.

Zifchock, R., Davis, I., Higginson, J., & Royer, T. (2008). The symmetry angle: A novel, robust method of quantifying asymmetry. *Gait & Posture, 27*(4), 622-627

APPENDIX A

INFORMED CONSENT FORM

ORP OFFICE USE ONLY

DO NOT REMOVE OR MODIFY

IRB# 36656 Doc. #1001

The Pennsylvania State University

Informed Consent Form for Biomedical Research
The Pennsylvania State University

Title of Project: Measurement of Arm Swing Using Video Based Motion Analysis and Accelerometry

Principal Investigator: Stephen J. Piazza, PhD
Biomechanics Laboratory
29 Recreation Building, University Park, PA 16802
814-865-3413; piazza@psu.edu

Other Investigator(s): Nancy Campbell, The Pennsylvania State University
Xuemei Huang, MD, PhD, The Pennsylvania State University
Joseph P. Cusumano, PhD, The Pennsylvania State University

This is to certify that you, _____, have been given the following information with respect to your participation as a volunteer in a program of investigation under the supervision of Dr. Stephen Piazza.

1. **Purpose of the study:** You are being asked to participate in a study being conducted in the Penn State Biomechanics Laboratory, which is a laboratory specializing in studies of human movement. The purpose of this study is to determine which of two methods of measurement, video based motion analysis or accelerometers, is able to most accurately measure arm swing while walking. Because the results of the study could be affected if the full purpose is known prior to your participation, the purpose of the study cannot be explained to you at this time. You will have an opportunity to receive a complete explanation purpose following completion of the study.

2. **Procedures to be followed:** Healthy participants between the ages of 18-40 years of age will participate in this study. You and the other volunteers will have measurements of both your height and weight taken. Wrist weights will be attached to each wrist. Several round markers about the size of a marble attached to hard plastic shells will be applied with adhesive tape to the skin at various locations on both of your arms as well as both hips. Accelerometers will be attached to each of your forearms with double-sided tape and elastic wrap. Accelerometers are electromechanical devices that measure dynamic accelerations.

   You will be asked to stand still for a few seconds while the cameras record the locations of the single markers near your joints.

   You will then be asked to walk approximately thirty feet at a comfortable pace while wearing wrist weights on each wrist. You will repeat this five times with each of ten different weight combinations while cameras record the locations of the markers on your arms and the accelerometers measure the dynamic accelerations of your armswing.

3. **Discomforts and risks:** There are only minimal risks associated with this study. There are no known risks associated with the wearing of markers on the skin or with recording

of your movements using the cameras. If you should experience any discomfort during these trials, please inform the researcher and you will be given an opportunity to rest or discontinue the experiment. If you feel that you cannot or should not perform any of these tasks, you should not participate in this study.

4. **Benefits:** There is no direct benefit to you for participating in this research. There is an indirect benefit of contributing to the development of a new method of measurement of arm swing in Parkinson's patients.

5. **Duration/time of the procedures and study:** Your visit to the Biomechanics Laboratory will last approximately 1 hour.

6. **Statement of confidentiality:** Any data collected in this experiment will remain confidential. The data will be located within a file cabinet in a part of The Biomechanics Lab that has limited access and will remain under the supervision of Dr. Stephen Piazza.

   Any identifiers, such as your name or personal information, will be kept separate from the actual data.

   All records associated with your participation in the study will be subject to the usual confidentiality standards applicable to medical records (e.g., such as records maintained by physicians, hospitals, etc.). In the event of any publication resulting from the research, no personally identifiable information will be disclosed.

   The Office of Human Research Protections in the U.S. Department of Health and Human Services, the U.S. Food and Drug Administration (FDA), the Office for Research Protections at Penn State and the Biomedical Institutional Review Board may review records related to this project.

7. **Right to ask questions:** You can ask questions about this research. Please contact Dr. Stephen Piazza at (814) 865-3413 with questions. You can also call this number if you have complaints or concerns about the research. If you have questions about your rights as a research participant, or you have concerns or general questions about the research, contact The Pennsylvania State University's Office for Research Protections at (814) 865-1775. The ORP cannot answer questions about research procedures. Questions about research procedures can be answered by the research team.

8. **Payment for participation:** You will not receive payment for participation in this study.

9. **Voluntary participation:** Your decision to be in this research is voluntary. You can stop at any time. You do not have to answer any questions you do not want to answer. Refusal to take part in or withdrawing from this study will involve no penalty or loss of benefits you would receive otherwise.

10. **Injury Clause:** In the unlikely event you become injured as a result of your participation in this study, medical care is available. It is the policy of this institution to provide neither financial compensation nor free medical treatment for research-related injury. By signing this document, you are not waiving any rights that you have against The Pennsylvania State University for injury resulting from negligence of the University or its investigators.

11. **Abnormal Test Results:** In the event that abnormal test results are obtained, you will be made aware of the results in ***3*** days and recommended to contact your private medical provider for follow-up.

You must be 18 years of age or older to take part in this research study. If you agree to take part in this research study and the information outlined above, please sign your name and indicate the date below.

You will be given a copy of this signed and dated consent for your records.

_____ _____

Participant Signature Date

_____ _____

Person Obtaining Consent Date

APPENDIX B

MATLAB CODE

```
clear all
close all
clc

% define segments
PELV = 1;
R_FA = 2;
L_FA = 3;

% define landmarks
R_LAT_ELB = 1;
R_MED_ELB = 2;
R_LAT_WRI = 3;
R_MED_WRI = 4;
L_LAT_ELB = 5;
L_MED_ELB = 6;
L_LAT_WRI = 7;
L_MED_WRI = 8;
R_ASIS    = 9;
L_ASIS    = 10;
R_PSIS    = 11;
L_PSIS    = 12;

% set to 1 for plotting cluster mkrs in anatomical frame
PLOT_FLAG = 0;

% set to 1 if you want missing motion trial markers to display
DISPLAY_MISSING = 0;

% this is the shortest unbroken string permitted for motion trials
SHORTEST_ALLOWED = 130;

% cutoff frequency for lowpass filtering of marker coordinates (Hz)
cutoff_freq = 7;

% max allowed intermarker distance SD
dist_sd_threshold = 2.0;

% user inputs filenames and pathname for standing trial
[fn,pn] = uigetfile('*.trc', 'Locate the TRC file with the standing trial');

% determine root of the filename
fn_root = fn(1:7);

% display progress to user
outstr = ['Processing standing trial file ' fn '...'];
disp(outstr)
```

```
48
49      % remember the starting directory
50 -    start_dir = pwd;
51
52      % go to the directory with the standing trial
53 -    cd(pn);
54
55      % open the TRC file and read in the marker locations
56 -    indata = importdata(fn,'\t',6);
57
58      % return to starting directory
59 -    cd(start_dir);
60
61      % copy markers into individual matrices
62 -    for mkr = 1:4
63 -        cluster_mkr(PELV,mkr).coords = indata.data(:,57+(mkr-1)*3:57+(mkr-1)*3+2);
64 -        cluster_mkr(R_FA,mkr).coords = indata.data(:,9+(mkr-1)*3:9+(mkr-1)*3+2);
65 -        cluster_mkr(L_FA,mkr).coords = indata.data(:,36+(mkr-1)*3:36+(mkr-1)*3+2);
66 -    end
67
68 -    anat_mkr(R_LAT_ELB).coords = indata.data(:,3:5);
69 -    anat_mkr(R_MED_ELB).coords = indata.data(:,6:8);
70 -    anat_mkr(R_LAT_WRI).coords = indata.data(:,24:26);
71 -    anat_mkr(R_MED_WRI).coords = indata.data(:,27:29);
72 -    anat_mkr(L_LAT_ELB).coords = indata.data(:,30:32);
73 -    anat_mkr(L_MED_ELB).coords = indata.data(:,33:35);
74 -    anat_mkr(L_LAT_WRI).coords = indata.data(:,51:53);
75 -    anat_mkr(L_MED_WRI).coords = indata.data(:,54:56);
76 -    anat_mkr(R_ASIS).coords = indata.data(:,72:74);
77 -    anat_mkr(L_ASIS).coords = indata.data(:,75:77);
78 -    anat_mkr(R_PSIS).coords = indata.data(:,78:80);
79 -    anat_mkr(L_PSIS).coords = indata.data(:,81:83);
80
81      % check for missing markers
82 -    for seg = PELV:L_FA
83 -        for mkr = 1:4
84 -            index_list = isnan(cluster_mkr(seg,mkr).coords);
85 -            for frm = 1:300
86 -                if (index_list(frm,1))
87 -                    outstr = ['Missing marker: Segment #' num2str(seg) ...
88                          ' Marker #' num2str(mkr) ' Frame #' num2str(frm)];
89 -                    disp(outstr)
90 -                end
91 -            end
92 -        end
93 -    end
94
```

```
for a_mkr = R_LAT_ELB:L_PSIS
    index_list = isnan(anat_mkr(a_mkr).coords);
    for frm = 1:300
        if (index_list(frm,1))
            outstr = ['Missing marker: Anatomical Marker #' ...
                num2str(a_mkr) ' Frame #' num2str(frm)];
            disp(outstr)
        end
    end
end

resp = input('Continue? ([y]/n): ','s');
if (isempty(resp))
    junk = 1;
elseif (resp == 'N' || resp == 'n')
    return
end

cluster_in_anatomical = zeros(3,300,4,3);

% for every frame
for fr = 1:300
    for seg = PELV:L_FA
        % define anatomical markers for each segment
        switch (seg)
            case (PELV)
                AMKR1 = anat_mkr(R_ASIS).coords;
                AMKR2 = anat_mkr(L_ASIS).coords;
                AMKR3 = anat_mkr(R_PSIS).coords;
                AMKR4 = anat_mkr(L_PSIS).coords;
            case (R_FA)
                AMKR1 = anat_mkr(R_LAT_WRI).coords;
                AMKR2 = anat_mkr(R_MED_WRI).coords;
                AMKR3 = anat_mkr(R_LAT_ELB).coords;
                AMKR4 = anat_mkr(R_MED_ELB).coords;
            case (L_FA)
                AMKR1 = anat_mkr(L_LAT_WRI).coords;
                AMKR2 = anat_mkr(L_MED_WRI).coords;
                AMKR3 = anat_mkr(L_LAT_ELB).coords;
                AMKR4 = anat_mkr(L_MED_ELB).coords;
        end

        % find Tga from anatomical marker coordinates in ground frame
        if (seg == PELV)
            MIDPT1 = (AMKR1(fr,:)+AMKR2(fr,:))/2;
            MIDPT2 = (AMKR3(fr,:)+AMKR4(fr,:))/2;
            orig = (MIDPT1+MIDPT2)/2;
```

```
142 -               x_u = mk_unit_vec(MIDPT2,MIDPT1);
143 -               q_u = mk_unit_vec(AMKR2(fr,:),AMKR1(fr,:));
144 -               y_u = cross(q_u,x_u);
145 -               z_u = cross(x_u,y_u);
146 -               Tga = [x_u' y_u' z_u' orig'; 0 0 0 1];
147 -           else
148 -               MIDPT1 = (AMKR1(fr,:)+AMKR2(fr,:))/2;
149 -               MIDPT2 = (AMKR3(fr,:)+AMKR4(fr,:))/2;
150 -               orig = (MIDPT1+MIDPT2)/2;
151 -               y_u = mk_unit_vec(MIDPT1,MIDPT2);
152 -               q_u = mk_unit_vec(AMKR2(fr,:),AMKR1(fr,:));
153 -               z_u = cross(q_u,y_u);
154 -               x_u = cross(y_u,z_u);
155 -               Tga = [x_u' y_u' z_u' orig'; 0 0 0 1];
156 -           end
157
158 -           wrist_ctr_a(seg).coords = inv(Tga)*[MIDPT1 1]';
159
160           % find Tgl from local (cluster) marker coordinates in ground frame
161 -           orig = cluster_mkr(seg,1).coords(fr,:);
162 -           x_u = mk_unit_vec(cluster_mkr(seg,1).coords(fr,:),...
163               cluster_mkr(seg,4).coords(fr,:));
164 -           q_u = mk_unit_vec(cluster_mkr(seg,1).coords(fr,:),...
165               cluster_mkr(seg,2).coords(fr,:));
166 -           z_u = cross(x_u,q_u);
167 -           y_u = cross(z_u,x_u);
168 -           Tgl = [x_u' y_u' z_u' orig'; 0 0 0 1];
169
170           % compute Tla = inv(Tgl) * Tga
171 -           Tla = inv(Tgl) * Tga;
172
173           % find Tal = inv(Tla)
174 -           Tal = inv(Tla);
175
176 %           if (seg==3 && fr==10)
177 %               outstr = [num2str(seg) ' ' num2str(fr)];
178 %               disp(outstr)
179 %               cluster_mkr(seg,1).coords(fr,:)
180 %               cluster_mkr(seg,2).coords(fr,:)
181 %               cluster_mkr(seg,3).coords(fr,:)
182 %               cluster_mkr(seg,4).coords(fr,:)
183 %               Tgl
184 %               Tla
185 %               pause
186 %           end
187
188
```

```
189         % use inv(Tgl) to get local markers in local frame Pl = inv(Tgl) * Pg
190         % compute coordinates of cluster markers in anatomical frame using
191         % Pa = Tal * Pl = Tal * (inv(Tgl) * Pg)
192 %         CMKR1_A = Tal * (inv(Tgl) * [cluster_mkr(seg,1).coords(fr,:)'; 1]);
193 %         CMKR2_A = Tal * (inv(Tgl) * [cluster_mkr(seg,2).coords(fr,:)'; 1]);
194 %         CMKR3_A = Tal * (inv(Tgl) * [cluster_mkr(seg,3).coords(fr,:)'; 1]);
195 %         CMKR4_A = Tal * (inv(Tgl) * [cluster_mkr(seg,4).coords(fr,:)'; 1]);
196
197 -         CMKR1_A = inv(Tga) * [cluster_mkr(seg,1).coords(fr,:)'; 1];
198 -         CMKR2_A = inv(Tga) * [cluster_mkr(seg,2).coords(fr,:)'; 1];
199 -         CMKR3_A = inv(Tga) * [cluster_mkr(seg,3).coords(fr,:)'; 1];
200 -         CMKR4_A = inv(Tga) * [cluster_mkr(seg,4).coords(fr,:)'; 1];
201
202         % store result for this frame
203 -         cluster_in_anatomical(seg,fr,1,:) = CMKR1_A(1:3);
204 -         cluster_in_anatomical(seg,fr,2,:) = CMKR2_A(1:3);
205 -         cluster_in_anatomical(seg,fr,3,:) = CMKR3_A(1:3);
206 -         cluster_in_anatomical(seg,fr,4,:) = CMKR4_A(1:3);
207 -     end
208 - end
209
210   % plot
211 - if (PLOT_FLAG)
212 -     for seg = PELV:L_FA
213 -         xx = squeeze(cluster_in_anatomical(seg,:,1,1));
214 -         yy = squeeze(cluster_in_anatomical(seg,:,1,2));
215 -         zz = squeeze(cluster_in_anatomical(seg,:,1,3));
216 -         plot3(xx,yy,zz,'r.'), hold on
217 -         xx = squeeze(cluster_in_anatomical(seg,:,2,1));
218 -         yy = squeeze(cluster_in_anatomical(seg,:,2,2));
219 -         zz = squeeze(cluster_in_anatomical(seg,:,2,3));
220 -         plot3(xx,yy,zz,'g.')
221 -         xx = squeeze(cluster_in_anatomical(seg,:,3,1));
222 -         yy = squeeze(cluster_in_anatomical(seg,:,3,2));
223 -         zz = squeeze(cluster_in_anatomical(seg,:,3,3));
224 -         plot3(xx,yy,zz,'b.')
225 -         xx = squeeze(cluster_in_anatomical(seg,:,4,1));
226 -         yy = squeeze(cluster_in_anatomical(seg,:,4,2));
227 -         zz = squeeze(cluster_in_anatomical(seg,:,4,3));
228 -         plot3(xx,yy,zz,'k.')
229 -         axis equal
230
231 -         pause
232 -         close all
233 -     end
234 - end
235
```

```
236     % average across frames to get cluster marker coordinates in anatomical
237     % frame
238 -   mean_clust_in_anat = zeros(3,4,3); % seg, mkr, coord
239 -   for seg = PELV:L_FA
240 -       for mkr = 1:4
241 -           for coord = 1:3
242 -               mean_clust_in_anat(seg,mkr,coord) = ...
243                     mean(squeeze(cluster_in_anatomical(seg,200:230,mkr,coord))); % 51:250
244 -           end
245 -       end
246 -   end
247
248     % find out which motion trials to process
249 -   trials = input('Which motion trials? (use brackets): ');
250 -   n_trials = length(trials);
251
252     % begin trial loop here
253 -   for tr = 1:n_trials
254
255         % which trial is this?
256 -       this_trial = trials(tr);
257
258         % go back to directory where standing trial was
259 -       cd(pn)
260
261         % user inputs filenames and pathname for motion trial
262 -       fn = [fn_root num2str(this_trial) '.trc'];
263
264         % display progress to user
265 -       outstr = ['Processing motion trial file ' fn '...'];
266 -       disp(' ')
267 -       disp(outstr)
268
269
270         % open the TRC file and read in the marker locations
271         % indata = importdata(fn,'\t',6);
272 -       nframes = 500;
273 -       indata.data = zeros(nframes,47);
274 -       fid = fopen(fn);
275 -       for ii=1:6, tline=fgets(fid);, end % skip past headerlines
276 -       for ii=1:500
277 -           zz = textscan(fid,'%f',47,'delimiter','\t'); % read first 47 values in this line
278 -           if (isempty(zz{1})) % have we reached the end of the file??
279 -               nframes = ii - 1;
280 -               break;
281 -           end
282 -           indata.data(ii,:) = zz{1}';
```

```
283 -           junk = textscan(fid,'%s',1,'delimiter','\n'); % read rest of line
284 -       end
285 
286         % reset size of indata
287 -       indata.data = indata.data(1:nframes,:);
288 
289         % return to starting directory
290 -       cd(start_dir);
291 
292         % copy markers into individual matrices
293 -       for mkr = 1:4
294 -           cluster_mkr(PELV,mkr).coords = indata.data(1:nframes,33+(mkr-1)*3:33+(mkr-1)*3+2)
295 -           cluster_mkr(R_FA,mkr).coords = indata.data(1:nframes,3+(mkr-1)*3:3+(mkr-1)*3+2);
296 -           cluster_mkr(L_FA,mkr).coords = indata.data(1:nframes,18+(mkr-1)*3:18+(mkr-1)*3+2)
297 -       end
298 
299         % find when all markers are present
300 -       marker_roster = ones(nframes,12);
301 -       for seg = PELV:L_FA
302 -           for mkr = 1:4
303 -               index_list = isnan(cluster_mkr(seg,mkr).coords);
304 -               for frm = 1:nframes
305 -                   if (index_list(frm,1))
306 -                       if (DISPLAY_MISSING)
307 -                           outstr = ['Missing marker: Segment #' num2str(seg) ...
308                                ' Marker #' num2str(mkr) ' Frame #' num2str(frm)];
309 -                           disp(outstr)
310 -                       end
311 -                       marker_roster(frm,(seg-1)*4+mkr) = 0;
312 -                   end
313 -               end
314 -           end
315 -       end
316 
317 -       curr_continuous = 0;
318 -       curr_start = 0;
319 -       best_so_far = 0;
320 -       best_start = 0;
321 -       best_end = 0;
322 -       for frm = 1:nframes
323 -           if (sum(marker_roster(frm,:)) < 12)
324 -               if (curr_continuous > best_so_far)
325 -                   best_so_far = curr_continuous;
326 -                   best_start = curr_start;
327 -                   best_end = frm - 1;
328 -               end
329 -               curr_continuous = 0;
```

```
330 -                   -
331 -           else
332 -               if (curr_continuous == 0)
333 -                   curr_start = frm;
334 -               end
335 -               curr_continuous = curr_continuous + 1;
336 -           end
337 -       end
338 
339 -       % did trial finish in middle of best string?
340 -       if (curr_continuous > best_so_far)
341 -           best_so_far = curr_continuous;
342 -           best_start = curr_start;
343 -           best_end = frm;
344 -       end
345 
346 -       outstr = ['Best unbroken string starts at fr #' num2str(best_start) ...
347 -           ' and ends at fr #' num2str(best_end)];
348 -       disp(outstr)
349 -       disp(' ')
350 
351 -       unbroken = best_end - best_start + 1;
352 -       if (unbroken < SHORTEST_ALLOWED)
353 -           disp('WARNING: Short unbroken string!!')
354 -           resp = input('Continue? ([y]/n): ','s');
355 -           if (isempty(resp))
356 -               junk = 1;
357 -           elseif (resp == 'N' || resp == 'n')
358 -               return
359 -           end
360 -       end
361 
362       %% cutoff frequency analysis
363 %       cols = 'bgrcmb';
364 %       for seg = R_FA:L_FA
365 %           for coord  = 1:3
366 %               for mkr = 1:4
367 %                   resids = zeros(14,1);
368 %                   figure(98), plot(cluster_mkr(seg,mkr).coords(best_start:best_end,coord), 'k-')
369 %                   figure(98), hold on
370 %                   for fc = 2:15
371 %                       data = cluster_mkr(seg,mkr).coords(best_start:best_end,coord);
372 %                       data_f = lowpass(data, 100, fc);
373 %
374 %                       if ((fc > 1) && (fc < 8))
375 %                           figure(98), plot(data_f, cols(fc-1))
376 %                           figure(98), hold on
```

```
%
%                   resids(fc-1) = sqrt((1/unbroken)*sum((data-data_f).^2));
%               end
%               figure(99), plot(2:15,resids,'bo-')
%               figure(99), hold on
%
%               figure(98), title(['SEG ' num2str(seg) ' COORD ' num2str(coord) ' MKR ' num2str(mkr)])
%               pause
%               close(98)
%           end
%       end
%   end
%
%   figure(99), xlabel('cutoff freq (Hz)')
%   figure(99), ylabel('RMSE (mm)')
%
%    pause

%%

euler_angles = zeros(seg,best_end-best_start+1,3);
origin_loc = zeros(seg,best_end-best_start+1,3);
wrist_ctr_g = zeros(seg,best_end-best_start+1,4);
wrist_pos = zeros(seg,best_end-best_start+1,3);
T = zeros(seg,best_end-best_start+1,4,4);

euler_angles_f = zeros(seg,best_end-best_start+1,3);
origin_loc_f = zeros(seg,best_end-best_start+1,3);
wrist_ctr_g_f = zeros(seg,best_end-best_start+1,4);
wrist_pos_f = zeros(seg,best_end-best_start+1,3);
T_f = zeros(seg,best_end-best_start+1,4,4);

for seg = PELV:L_FA
    a_mkrs = squeeze(mean_clust_in_anat(seg,:,:))';

    for mkr = 1:4
        for coord = 1:3
            data = ...
                cluster_mkr(seg,mkr).coords(best_start:best_end,coord);
            cluster_mkr_f(seg,mkr).coords(best_start:best_end,coord)= ...
                lowpass(data, 100, cutoff_freq);
        end
    end

    % use intermarker distances to check cluster rigidity
    for mkr1 = 1:3
        for mkr2 = mkr1+1:4
```

```
                m1 = squeeze(cluster_mkr_f(seg,mkr1).coords(best_start:best_end,:));
                m2 = squeeze(cluster_mkr_f(seg,mkr2).coords(best_start:best_end,:));

                this_dist = ((m2(:,1)-m1(:,1)).^2 + (m2(:,2)-m1(:,2)).^2 + ...
                    (m2(:,3)-m1(:,3)).^2).^0.5;
                this_dist_sd = std(this_dist);
                outstr = sprintf('seg = %i m1 = %i m2 = %i SD = %10.2f', ...
                    seg, mkr1, mkr2, this_dist_sd);
                if (this_dist_sd > dist_sd_threshold)
                    outstr = [outstr ' WARNING: Possible non-rigid cluster'];
                end
                disp(outstr);
            end
        end

        for frm = best_start:best_end
            b_mkrs = zeros(3,4);
            b_mkrs_f = zeros(3,4);

            for mkr = 1:4
                b_mkrs(:,mkr) = cluster_mkr(seg,mkr).coords(frm,:);
                b_mkrs_f(:,mkr) = cluster_mkr_f(seg,mkr).coords(frm,:);
            end

            Tga = lsqRT(a_mkrs,b_mkrs);
            Tga_f = lsqRT(a_mkrs,b_mkrs_f);

            T(seg,frm-best_start+1,:,:) = Tga;
            T_f(seg,frm-best_start+1,:,:) = Tga_f;

            euler_angles(seg,frm-best_start+1,:) = (180/pi)*...
                ZYX_decomp(Tga(1:3,1:3));
            euler_angles_f(seg,frm-best_start+1,:) = (180/pi)*...
                ZYX_decomp(Tga_f(1:3,1:3));

            origin_loc(seg,frm-best_start+1,:) = Tga(1:3,4)';
            origin_loc_f(seg,frm-best_start+1,:) = Tga_f(1:3,4)';

            if (seg > PELV)
                wrist_ctr_g(seg,frm-best_start+1,:) = ...
                    Tga*wrist_ctr_a(seg).coords;
                wrist_ctr_g_f(seg,frm-best_start+1,:) = ...
                    Tga_f*wrist_ctr_a(seg).coords;

                wrist_pos(seg,frm-best_start+1,:) = ...
                    squeeze(wrist_ctr_g(seg,frm-best_start+1,1:3)) - ...
                    squeeze(origin_loc(PELV,frm-best_start+1,:));
```

```
471 -                   wrist_pos_f(seg,frm-best_start+1,:) = ...
472                         squeeze(wrist_ctr_g_f(seg,frm-best_start+1,1:3)) - ..
473                         squeeze(origin_loc_f(PELV,frm-best_start+1,:));
474 -               end
475 -           end
476 -       end
477
478 -       disp('Finished processing motion trial.  Saving ...')
479
480         % save output for this trial
481 -       out_fn = [fn_root num2str(this_trial) '.mat'];
482 -       cd(pn)
483 -       save(out_fn,'euler_angles','origin_loc','wrist_ctr_g','wrist_pos','T'
484 -       cd(start_dir)
485
486 -       disp('Saved.')
487 -       disp(' ')
488 - end
489
```

APPENDIX C

TABLE OF CONDITIONS

Condition	Mass Left (g)	Mass Right (g)
1	0	0
2	400	0
3	350	50
4	300	100
5	250	150
6	200	200
7	150	250
8	100	300
9	50	350
10	0	400

Academic Vita of Nancy M. Campbell

nmc5104@psu.edu

Education:

- B.S. Kinesiology, Movement Science, May 2012
  The Pennsylvania State University; University Park, PA

Professional Experience:

Clinical Shadowing; Smithtown, NY **June 2009 – Aug 2009**

- Actively studied doctor-patient interaction in private office
- Learned to filter family history and conduct range of motion testing
- Observed various orthopedic surgical procedures

Anatomy Teaching Assistant; University Park, PA **Jan 2010 – May 2010**

- Used human cadavers to teach functional anatomy to college freshmen, sophomores, and juniors
- Supervised classroom activities to ensure participation by all students

Biology Peer Mentor; University Park, PA **Aug 2009 – Dec 2010**

- Guided four freshmen enrolled introductory biology on successful note taking and study habits
- Reinforced challenging concepts in weekly classroom meetings

Biology Teaching Assistant; University Park, PA **Aug 2010 – Dec 2011**

- Supervised freshmen in introductory biology laboratory techniques
- Reinforced challenging concepts during laboratory sessions

Tutor; University Park, PA **Nov 2010 – July 2011**

- Tutored collegiate student athletes in general chemistry, organic chemistry, biology, physiology, and anatomy courses

Academic Researcher **Nov 2008 - Present**

- Co-investigator on honors thesis project
- Completed IRB, developed protocol, and collected data

Academic Awards:

- Schreyer Honors Scholar **August 2009 – Present**
- Dean's List recipient 7 out of 7 Semesters **December 2008 – Present**
- Golden Key International Honor Society **December 2010 – Present**
- Phi Kappa Phi Honor Society **March 2012 – Present**